State-Resolved Studies of Reactions in the Gas Phase

C. Bradley Moore*

Department of Chemistry, University of California at Berkeley and Chemical Sciences Division, Lawrence Berkeley National Laboratory, Berkeley, California 94720-1460

Ian W. M. Smith

School of Chemistry, The University of Birmingham, Edgbaston, Birmingham B15 2TT, United Kingdom

Received: December 8, 1995; In Final Form: April 10, 1996[⊗]

During the first years of *The Journal of Physical Chemistry*, chemists were just beginning to understand chemical reactions in gases as sequences of elementary reaction steps. Basic models of reaction dynamics were developed in succeeding decades which provided powerful qualitative insight into reaction mechanisms and rate constants. In recent decades, the development of molecular beam and laser technologies has allowed us to look into the transition state region at the dynamics of chemical bond formation and breaking. State-selective preparation of reactants and state-resolved detection of products with velocity and angle resolution permit exacting quantitative test of dynamical theories. Thanks to the ability to calculate accurate *ab initio* potential energy surfaces and solve Schroedinger's equation for reactive scattering dynamics, the simplest reactions are now understood quantitatively at the most fundamental level possible. The concepts and models thus developed, along with ever more powerful experimental and computational tools, are rapidly being applied to more complex reactions.

Introduction

During the present century, physical chemists have striven to obtain an ever deeper understanding of chemical reactivity. At the end of the 19th century, chemical kineticists, with primitive tools but amazing perspicacity, began to realize that observable chemical changes often took place not in a single universal transformation but via a network of what we now call elementary reactions. This marvelous work is exemplified by Bodenstein's discovery of the chain mechanisms of the reactions between H_2 and the diatomic halogens,[1] still taught in most undergraduate courses on chemical kinetics.[2]

A gradual appreciation that elementary reactions are of vital importance, both from a fundamental viewpoint and for the practical understanding of complex systems, led to efforts to study their rates in isolation. Here, "in isolation" carries two connotations. First, every effort is made to ensure that the effect one is measuring results only—or at least predominantly—from the chosen elementary reaction.[3] Second, such considerations favor gas-phase studies since then every contribution to the reaction arises from an event involving *one* (*unimolecular* reaction), *two* (*bimolecular* reaction), or *three* (*termolecular* reaction) molecules. In the gas phase, there is no need to worry about interactions between reagent and solvent molecules, and so these important interactions and their effects on chemical reactions are left to other authors in this special issue.[4,5]

Studies of the kinetics of elementary reactions and the mechanisms of complex reactive systems have grown steadily in importance. Today, computing power allows us to tackle much more complex systems than in the past: complicated combustion processes,[6] the atmospheres of Earth and other planets,[7] and interstellar clouds.[8,9] For all these hugely complicated environments, a rather different approach is used from that adopted in early laboratory studies. Rather than infer the mechanisms, and maybe the rates of some of the individual steps from observations of the changes in the concentrations of the major participating species, one can now model a complex system "bottom up", in today's terminology, by computing the anticipated overall change resulting from a huge network of chemical and photochemical elementary steps whose rate constants have been evaluated in the laboratory.

The acquisition of reliable rate constants for elementary reactions proceeding under conditions of thermal equilibrium started in the 1950s and early 1960s. For bimolecular reactions at least, this advance was brought about by the development of pulsed-photolysis and discharge-flow techniques which could not only generate radical species but also give sufficient time resolution and observational sensitivity for reaction rates to be measured. Although flash lamps have now been replaced by pulsed lasers and detection methods have developed apace, these two general methods remain central to the kinetic study of elementary reactions.[2,3]

Early pulsed photolysis experiments also began to reveal more detailed features of elementary reactions than their rate constants and the dependence of those rate constants on temperature. For example, chemical and photochemical products (e.g., O_2 formed in the $O(^3P) + NO_2$ reaction and by photodissociation of O_3) were observed over a range of vibrationally excited states.[10] It was realized that such observations—and many others—could allow the chemist to infer what goes on during the fleeting instant in which a molecule (or two molecules in a binary collision) change the nature of their chemical bonding in such a way as to form new species.

The 1960s and early 1970s saw the founding of "molecular reaction dynamics" as a distinct field within physical chemistry. The sequence of *Faraday Discussions* between 1962 and 1973 serve as valuable milestones.[11−13] It had been appreciated since the 1930s that potential energy surfaces, describing the interactions between individual atoms, were crucial in determining the dynamical behavior in stable molecules (i.e., ones whose internal kinetic energy is less than the lowest dissociation limit), in unstable molecules (where the kinetic energy is sufficient to bring about dissociation or isomerization), and in molecular

[⊗] Abstract published in *Advance ACS Abstracts,* June 15, 1996.

S0022-3654(95)03664-1 CCC: $12.00

collisions. With enormous effort and no little ingenuity, potential energy surfaces (PES) had been constructed[14] and some trajectories had been calculated in the 1930s.[15] Then in the 1960s, the arrival of significant computing power transformed our ability to calculate trajectories, i.e., to simulate collisions involving a limited number of atoms (usually three) by solving the classical equations of motion.[16−24] Large enough samples of trajectories could be run to yield statistically meaningful results, and we could see how dynamical properties (e.g., cross section, product energy distributions, center-of-mass scattering angles) depend on features of the potential energy surface and on the kinematic properties of the system (i.e., the relative masses of the participating atoms).[25]

On their own, the impact of these theoretical results might have been limited. But this period saw the development of crossed molecular beam methods[26,27] and of sensitive spectroscopies (initially infrared chemiluminescence)[28,29] to interrogate the initial distributions of product molecules over rovibrational states. Together the experiments and calculations established some important paradigms: among them the ideas of *direct* reactions and those proceeding via *collision complexes*. Originally formulated for bimolecular reactions, with the rotation period of the whole system adopted as a clock and the symmetry of angular scattering as a measure, these limiting behaviors were clearly connected to the form of the potential energy surface: in particular, whether there was a deep potential energy well to "trap" the system. Now it is appreciated that there may be a whole spectrum of dynamical behavior: for example, "complexes" may survive for several vibrational periods but still fragment in a time much less than that required for a rotation.

Experimental studies of unimolecular and often bimolecular reactions now start with laser photons to select well-defined initial reactant states and finish with lasers to probe individual product quantum states. From today's perspective, it is salutary to recall that much of our understanding of molecular reaction dynamics is based on experiments which made no use of lasers of any kind. Indeed, the influence of lasers in the 1960s was indirect: reactions were sought which gave products in inverted population distributions so that they could form the basis for chemical lasers.[30,31] Nowadays the influence of the laser in experimental reaction dynamics is pervasive. They find a number of applications which make use of their power, short pulse widths, high spectral brightness, polarization, and tunability.[32]

They are used to generate atoms (especially H or D atoms) photochemically with defined velocities and molecules in selected internal energy states and, on occasion, with a defined plane of rotation. With tunable nanosecond lasers, molecular rovibronic energy states can be selected with a resolution of a few hundredths of a cm^{-1}. Picosecond lasers with line widths limited by the uncertainty principle resolve vibronic levels and prepare coherent ensembles of rotational levels. The shortest laser pulses, ~10 fs, can record the atomic motions as chemical bonds break in real time.[33−35] These femto- and picosecond lasers have revolutionized the study of direct dissociation on repulsive PES and reactions in condensed phases.[5,36,37] For unimolecular reactions on ground state PESs, the reactant lifetime is very long compared to the time needed to cross through the transition state along the reaction coordinate. The use of nanosecond lasers to give an indirect but clear view of dynamics in the transition state region by measuring rate constants and product energy state distributions as a function of reactant initial state is described below.

Tunable lasers also form the basis for an ever-increasing range of sophisticated spectroscopies (most with their accompanying acronym): e.g., laser-induced fluorescence (LIF), resonance-enhanced multiphoton ionization (REMPI), reactive ion imaging, coherent anti-Stokes Raman scattering (CARS), etc. They allow the (simple) products of unimolecular and bimolecular reactions to be interrogated at an amazing level of detail: product state distributions, translational velocities, preferred directions of rotation, etc. Reviews of modern experimental techniques in reaction dynamics can be found elsewhere in this issue.[32] We concentrate below on some of the conclusions reached.

As well as lasers, methods based on supersonic expansions have found widespread use in recent experimental studies of reaction dynamics. In uncollimated "free jets", the main advantage is the dramatic cooling which leads to greatly decreased populations in all but a few internal energy states. This enables the internal energy state of molecules excited by photon absorption to be better specified and also helps in defining the relative velocity of photofragments. With collimation, the expansion from supersonic nozzles produces intense molecular beams of well-defined velocity, allowing collision energies to be accurately specified in scattering experiments. Further, if the sources rotate around a common center, the relative velocity can be varied continuously,[38,39] and the product yields and product state distributions can be examined as a function of collision energy.[40]

Of course experimental limitations remain. As is shown in the main body of this article, for some prototypical unimolecular and bimolecular reactions involving small molecular species, the level of detail and the depth of understanding which the measurements reveal now approach the limits allowed by the quantum theory. However, this understanding is based almost entirely on the spectroscopic observation of atoms and diatomic molecules. Surely the methods of molecular reaction dynamics (theoretical, as well as experimental) are poised to "attack" chemically more complex systems.

Theoreticians, their ingenuity fueled by ever-increasing computer power, have also traveled a long way since the 1960s. *Ab initio* calculations now predict barrier heights for different reaction products and the geometries and frequencies of the transition state along the reaction path to each product with chemically useful accuracy.[41] For a time, the development of trajectory methods for investigating molecular processes overshadowed transition state theory, which had been the workhorse of theoretical chemical kinetics since its introduction in the 1930s.[42,43] This eclipse was, however, only temporary. A thorough reexamination of the basis of the theory[44] and indeed its close relationship to more overtly dynamical theories,[45] along with the development of microcanonical and vibrationally adiabatic versions and the examination of tunneling effects, reestablished transition state theory in its rightful place in the hierarchy of theories used to understand chemical processes.[46,47]

The theory is especially useful in its RRKM form for unimolecular reactions.[48−50] RRKM theory is, in effect, a microcanonical ensemble version of transition state theory. One of its basic postulates is that intramolecular energy flow is complete and rapid so that, for an excited molecule of a particular total energy (E) and angular momentum (J), all states are equally probable, and the microcanonical rate constant is then given by

$$k(E,J) = W(E,J)/h\rho(E,J) \qquad (1)$$

where $W(E,J)$ is the number of accessible and "active" internal states associated with motions orthogonal to the reaction coordinate at the transition state, $\rho(E,J)$ is the density of active states in the molecule, and h is Planck's constant. The assumption of rapid and complete intramolecular energy transfer

has been subject to numerous searching experimental tests over the past 25 years and has been found to be remarkably robust.[51] Very recently, experiments have confirmed the stepwise increase in $k(E,J)$ just above threshold:[52,53] as energy increases, $W(E,J)$ increases by one as each state (or "doorway") for reaction opens.

Transition state theory can also explain, in at least semiquantitative fashion, the influence of increasing the vibrational energy of reagents on exothermic bimolecular reaction rates via vibrationally adiabatic transition state theory.[46] Exothermic reactions have early barriers so the assumption of adiabaticity is valid, and increasing the state of vibration along the breaking bond will decrease the adiabatic barrier and lead to an enhancement of the reaction rates.

A crucial shortcoming of transition state theory is its inability to predict properties of the reaction products which largely depend on the form of the potential energy surface "beyond the transition state". A second problem is how one treats the results of collisions at a selected (high) collision energy. Now scattering calculations (possibly wedded to transition state methods) must be performed. A recent development of great importance has been the ability to carry out such calculations accurately using the equations of quantum, not classical, mechanics.[54] Nevertheless, the quasiclassical trajectory method (in which the initial internal energies of molecular reagents are chosen to correspond to those of the quantum states) appears to work remarkably well.[55] Only at a quite detailed level does it fail. Of course, to compare the results of the two types of calculation does not require a potential energy surface of special accuracy. But comparison of both sets of theoretical results with experiment does—the molecules in the experimental situation know the real potential! Experiment and quantum scattering calculations have become so accurate that differences are being blamed on small faults in the potential energy surface. Examples are given below.

In the next two sections of this article, we consider separately unimolecular and bimolecular reactions. Our strategy is to pick prototypical systems in order to examine closely our present stage of knowledge, where appropriate in an historical context. Some emphasis is placed on the underlying and crucial role which the potential energy surfaces play in molecular reaction dynamics. Although this article gives primarily an experimental perspective, it should be emphasized that advances in our understanding of reaction dynamics have resulted from concurrent and collaborative advances in theory[47,55] and experiment.

Unimolecular Reactions

RRKM theory has been widely applied to unimolecular reactions on ground state PESs.[48−50,56] During the past decade, it has progressed from a useful framework for fitting data with adjustable parameters to a quantitatively predictive theory using parameters determined by *ab initio* computation and spectroscopic experiments. RRKM theory incorporates the fundamental assumptions of TST that there is a local equilibrium between reactants and molecules crossing the transition state toward products along the reaction coordinate and that every molecule passing through the transition state proceeds to products without recrossing. RRKM theory is based on the additional assumptions that all vibrational states in the excited molecule are equally probable and that vibrational energy flows freely among the different degrees of freedom at a rate much faster than the reaction rate. RRKM theory presumes that motion along the reaction coordinate is classical and is decoupled from the bound vibrational motions at the transition state. The passage through the transition state is then vibrationally adiabatic, and the vibrational levels are defined over a sufficiently broad region near the transition state to give well-defined reaction thresholds or quantized channels connecting reactant to products. The microcanonical rate constant, proportional to the number of open channels $W(E,J)$, is thus predicted to increase stepwise as the energy increases through each vibrational level or threshold at the transition state, eq 1.

This step structure in $W(E,J)$ is apparently not an artifact of treating motion along the reaction coordinate classically since the quantum treatments of cumulative reaction probabilities (CRP)[57−59] exhibit quite similar structures. An elegant treatment of the exact quantum theory of chemical reaction rates[57] expresses the CRP as a sum of eigenvalues corresponding to the transition state theory sum of states. The stepped structure of the transition state theory expression for $k(E,J)$ is found in the exact quantum CRP as a function of E and J. For bimolecular reactions this structure is smoothed out when summation over total angular momentum states (or integration over impact parameter in classical terms) is carried out.[60] In practicable experiments further smoothing is caused by averaging over the spread in relative translational energy of the reactants. However, for unimolecular reactions with E and J defined, the microcanonical rate is directly proportional to the exact quantum CRP or more approximately to $W(E,J)$ corrected for one-dimensional tunneling through the barrier. Thus, the influence of transition state structure and dynamics on reaction rates and product energy state distributions can be resolved most clearly for unimolecular reactions. With the resolution of modern laser experiments in cooled, pulsed jets it is not necessary to average over total angular momentum and energy, and a form of spectroscopy is possible in which the energies of the vibrational levels of the transition state are revealed by steps in the rate constant as a function of energy.

The transition state gives the initial conditions for the dynamics of energy release in the repulsive exit valley of the potential energy surface.[61,62] The peaks of product energy state distributions are determined by the geometry of the transition state and the shape of the PES in the exit valley. The shapes of distributions are determined by the atomic positions and momenta at the transition state, that is, by the vibrational wave function of the molecule as it passes through the transition state. Consequently, if one looks in the wings of the distribution of a particular product quantum number, one expects to see increases in product yield as the energy passes through the threshold for excitation of a transition state vibration which contributes strongly to that product degree of freedom. This can provide a dynamically biased spectroscopy useful for picking out energy levels for specific transition state vibrations.[52,53]

The discussion above has implicitly assumed that the transition state, or point of no return, for a reaction is unambiguously located at the top of a single barrier along the reaction coordinate, a saddle point on the multidimensional PES (Figure 1). There are important classes of unimolecular reactions which do not have this shape of PES.[63] For example, the rupture of a single bond to form two free radicals usually has no barrier to the recombination of those radicals and hence no saddle point or repulsive exit valley (Figure 2).[64] Thus, there is a conceptual problem in defining and locating a transition state. In this case, a transition state may be defined separately for each adiabatic or effective potential. In the simplest case, the effective potential and the electronic potential along the reaction coordinate only differ by the inclusion of a centrifugal term, and the transition state is placed at the centrifugal maximum. In this extreme limit of the loose transition state, phase space theory (PST), $W(E,J)$ is given simply by the rotation−vibration energy levels of the product molecules added to the energy of the centrifugal

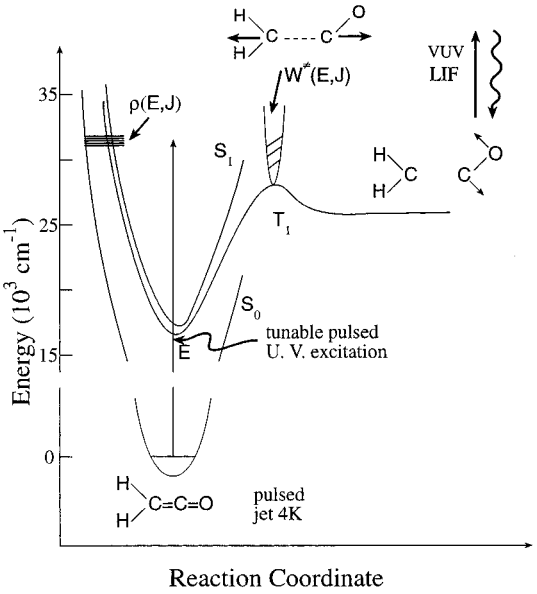

Figure 1. Dissociation of triplet ketene. The reaction coordinate is the distance between the carbon atoms. The solid lines represent the PES for the ground singlet (S_0), the first excited singlet (S_1), and the first triplet (T_1) electronic states. The transition state, which separates the highly vibrationally excited reactant from the products, is depicted as a single potential well perpendicular to the reaction coordinate. This well is meant to represent the eight bound vibrational coordinates at the transition state.

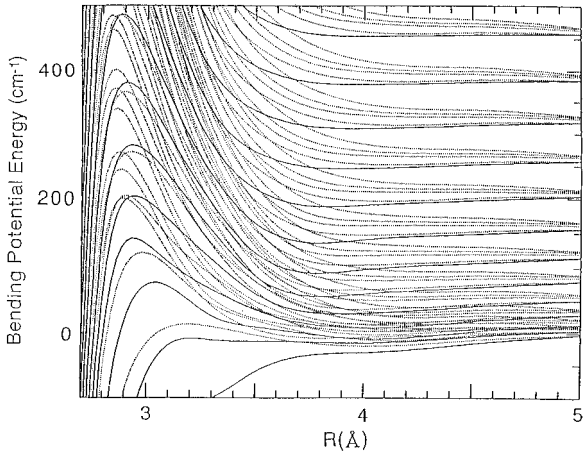

Figure 2. Adiabatic channels for a reaction with no barrier to recombination. Potential energy curves are shown for the energy levels of the bending vibrational motion of NO_2 for the lowest potential surface. The dotted lines show those for the excited state potential surfaces dissociating to the $NO(^2\Pi_{1/2}) + O(^3P_2)$ limit.[64]

barrier.[65] Exactly at threshold, there is only one channel open and PST must give an accurate rate constant. However, as energy increases, the number of product channels increases rapidly, in fact, much more rapidly than do the observed rate constants. This may be understood in terms of the increased spacing between energy levels as the product molecules approach along the reaction coordinate and free rotations become hindered rotations, then torsions, and ultimately bending vibrations of the reagent molecule.[50,66−68] If product channels are followed along the reaction coordinate back toward the stable reactant, one gets a family of noncrossing channel potentials for each rovibrational symmetry. In the variational RRKM theory,[66,67] one locates the transition state by searching along the reaction coordinate for the point at which the number of open channels at a given total energy is a minimum. This locates the transition state where the reactive flux is most limited; the transition state moves in along the reaction coordinate as the total energy increases above threshold. The statistical adiabatic channel model (SACM)[68] uses these same channel potentials and calculates the reaction rate constant by counting the number of channels with maxima at or below the total energy available.

In principle, these two theories must give identical rate constants when they use the same set of noncrossing channel curves. In practice, there are differences because different forms of the adiabatic channel curves are used or because the dynamics are assumed to jump across narrowly avoided crossings. It is generally agreed that product state vibrational quantum numbers are conserved through avoided crossings leading to different product vibrational states.[63,69,70] When variational RRKM theory is applied without this constraint, it gives rate constants which are too large. SACM is a dynamical theory as well as a rate theory and therefore predicts product energy state distributions. For completely adiabatic dynamics on noncrossing curves, the open channels correlate to the lowest open product states. However, if the assumption of rigorous adiabaticity is set aside, curves in the transition state region may be correlated to product states up to the limit imposed by conservation of energy and angular momentum. Since there is no repulsive exit valley to push the product fragments apart rapidly, the dynamics of energy flow as the molecule moves along the reaction coordinate between the transition state and the separated product fragments can be complicated. For total energies sufficiently close to threshold that PST is valid, the product energy state distributions must be statistical, with all open channels equally probable. The rate constants must then increase stepwise at the threshold energy for each product energy state.

Bond Breaking over a Barrier. The stepwise increase in rate constant with energy implied by eq 1 has been observed for the dissociation of ketene over a barrier on its triplet PES,[52,53]

$$CH_2CO \rightarrow {}^3CH_2 + CO$$

This process[53] is illustrated in Figure 1, which also shows the *ab initio* geometry[71,72] of ketene at this transition state. The *ab initio* calculations predict that the lowest frequency is for the torsion about the C−C bond and that the CCO bend and CH_2 out-of-plane wag are the next lowest. Hence, these modes are expected to dominate the structure of $k(E)$ in the first few hundred wavenumbers above threshold. Electronic−vibration couplings, internal conversion and intersystem crossing are sufficiently strong that the wave function of the excited molecule may be considered to be a statistical mixture of S_0, T_1, and S_1 basis states of comparable total energy. The density of vibrational states, counting all three electronic states, is essentially that of the ground state. The UV spectrum is smooth and flat.[73−75] Thus, as a UV exciting laser is tuned, it produces a constant number of hot ketene molecules ready to react along any accessible channel.

The rate constant data of Figure 3 were obtained by UV excitation of ketene cooled to 4 K in a pulsed jet.[53] A VUV pulse probed the CO product over a range of delay times to measure the product rise time. The observed thresholds give barrier heights above product zero-point energies of 1281 ± 15 cm^{-1} for CH_2CO and 1071 ± 40 cm^{-1} for CD_2CO, some 40% less than *ab initio* calculation.[52,53] Thus, deuteration gives a change in zero-point energy at the transition state of 1096 ± 20 cm^{-1} compared to the theoretical prediction of 1091 cm^{-1}. A torsional barrier of 240 cm^{-1} (35% less than that calculated *ab initio*) fits the positions of many steps for CH_2CO and CD_2-CO. The CCO bending vibration is observed at 250 cm^{-1} compared to an *ab initio* value of 252 cm^{-1}.[53] Other bending modes are observed at frequencies somewhat lower than

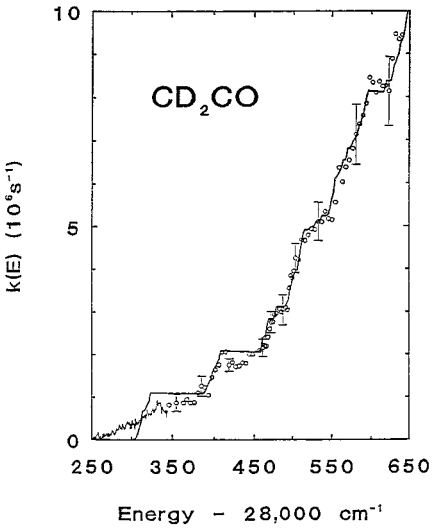

Figure 3. Stepped structure in the rate constant for CD_2CO dissociation as a function of the photolysis energy. The CO(v=0,J=12) PHOFEX curve ($\Delta t = 1.7\mu$s) is shown in the reaction threshold region; its intensity is arbitrarily scaled. The solid line is a RRKM fit.[53]

calculated. Couplings among vibrational modes and to the *a*-axis rotation appear to be important features of these low-frequency transition state vibrational modes.

In the application of RRKM theory, it is usually assumed not only that all vibrational degrees of freedom of a molecule are strongly mixed but also that Coriolis coupling mixes in the K_a degree of freedom.[50] To test this hypothesis for ketene, measurements were made as a function of jet temperature. For the cold ground state at 4 K, several J levels are populated, but only the lowest K_a levels of each nuclear spin symmetry, $K_a = 0, 1$, are populated. When the molecule is excited, strong K_a mixing causes all K_a values up to the limit of $\pm J$ to be equally populated. The associated energy locked up in rotation as the molecule crosses the transition state is $A^{\ddagger}K_a^2$, where $A^{\ddagger}$ is the *a*-axis rotational constant at the transition state. At a jet temperature of 30 K, zero to many tens of cm^{-1} of additional energy is required to cross through any particular vibrational threshold. The result of *K*-mixing would be a significant decrease in rate constant with increasing jet temperature. The observed rates were almost identical at 4 and 30 K, while the RRKM model predicts differences of up to 20% for K_a mixed. Thus, for values of $J \leq 6$, K_a appears to be a nearly good quantum number for highly excited ketene.[53]

The step heights in Figure 3 give the density of states for ketene, or more precisely the density divided by the effective triplet degeneracy at the transition state, $1 \leq g_t \leq 3$. It is not currently known how many of the three symmetries of triplet spin sublevels are coupled strongly to the singlet levels by intersystem crossing. The data for CH_2CO are accurately fit by $\rho = 1.11 g_t \rho_{WR}$ and for CD_2CO by $\rho = 1.19 g_t \rho_{WR}$.[53] There is ample precedent[76−78] for the density of levels of molecules of comparable size to be a factor of 3 (as would be implied by $g_t = 3$) to 10 larger than ρ_{WR} calculated using the Whitten−Rabinovitch[79] approximation. It will be necessary to understand and to be able to predict these unexpectedly large densities of states in order for RRKM theory to be completely quantitative and predictive.

There are significant discrepancies in detail apparent between eq 1 and the data for triplet dissociation of ketene. The slope of the step at threshold is rather gradual compared to those at higher energy. The $k(E)$ curves actually show modest peaks, whereas $W(E,J)$ corrected for 1-dimensional tunneling can only increase monotonically with energy. In a fully quantum

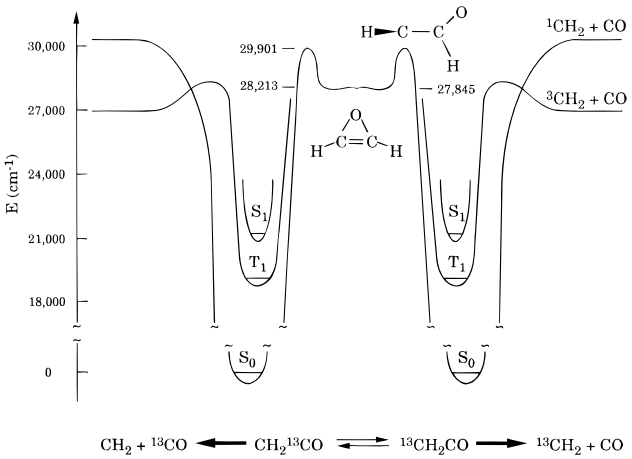

Figure 4. Potential energy diagram for all three unimolecular reactions of ketene with detailed[84] structures and energies for the C atom exchange isomerization.

treatment the steps in the rate constant are smoothed out completely, no steps or peaks, by tunneling through the *ab initio* barrier. This conclusion was unchanged by considering coupling of the C−C stretching reaction coordinate to the CCO bend or torsional coordinates.[80] A more complete knowledge of the potential function is needed in the region of the transition state and in the region where the reaction coordinates along the S_0 and T_1 surfaces diverge toward their asymptotic HCH angles for singlet and triplet CH_2. The reaction discussed in the following section provides a dramatic illustration of the importance of the detailed shape of the potential function along the reaction coordinate.

The dissociations of free radicals are important steps in many chemical processes. An ingenious method has recently been demonstrated for sensitive observation of the dynamics of free radical dissociations.[81] The anion of a radical is produced at low temperature in a pulsed jet and accelerated to high energy electrostatically. The electron is photodetached by one laser pulse to yield a neutral radical that is then photodissociated by a second laser pulse. The fragments move apart with relative velocity and angle determined by the fragmentation dynamics and impact with several kiloelectronvolts of energy on a position-sensitive multichannel plate. They are detected as correlated pairs with nearly unit efficiency. The fragment energy distributions observed[81] for

$$CH_2CHO \rightarrow CH_3 + CO$$
$$\rightarrow H + CH_2CO$$

indicate that dissociation follows internal conversion to the ground state PES. The minor channel, $CH_3 + CO$, was characterized in detail. This powerful new method of imaging the products of the dissociation of free radicals should rapidly advance our understanding of these important processes.

Isomerization Reactions. Isomerization reactions necessarily have substantial barriers and thus clearly defined transition states between stable valence isomers. Carbon atom exchange is one of three different unimolecular reactions of ketene with thresholds that lie within an energy range of 2000 cm^{-1} (Figure 4).[82] The molecule must pass through the highly strained three-membered ring geometry of oxirene in which the carbon atoms are equivalent.[83,84] At energies well above threshold, the measured reaction rates are fit accurately by RRKM theory with the transition state frequencies equal to the *ab initio* frequencies of oxirene.[85] Near the threshold, the rate constant exhibits a series of distinct peaks and valleys (Figure 5).[82] The coarse

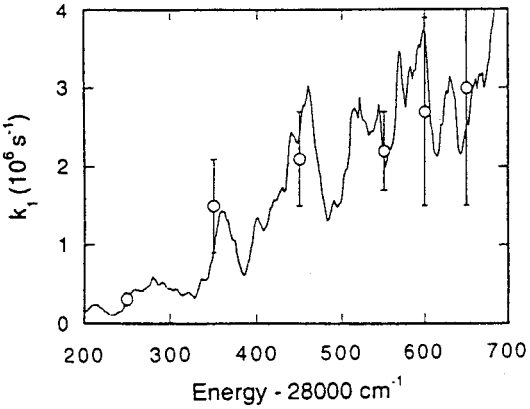

Figure 5. Rate constant for the isomerization $^{13}CH_2CO \rightarrow CH_2{}^{13}CO$ in the threshold region. The solid curve is from PHOFEX spectra of ^{12}CO and ^{13}CO products. All peaks of 0.2×10^{-6} s^{-1} and larger are completely reproducible. The points are direct time evolution measurements with 2σ error bars.[82]

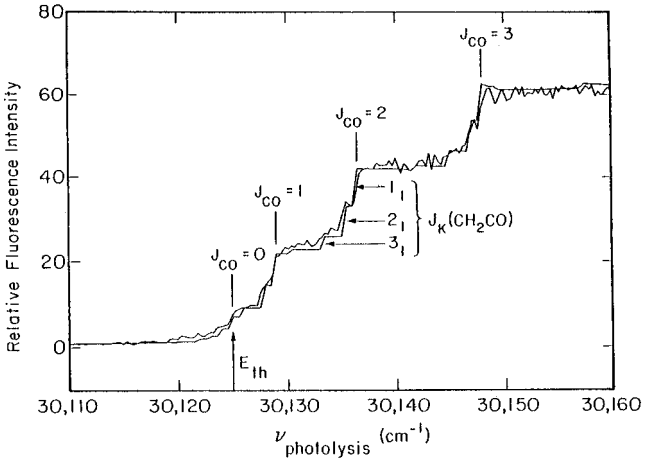

Figure 6. PHOFEX spectrum of the lowest rotational state of *ortho* singlet methylene near the threshold for $CH_2CO \rightarrow {}^1CH_2 + CO$. The smoother line is the phase space theory rate constant. The step positions match the rotational energy levels for free CO.

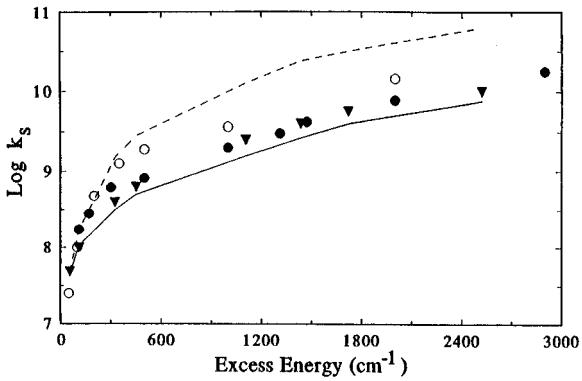

Figure 7. Energy dependence of the dissociation rate constant (s^{-1}) for $CH_2CO \rightarrow {}^1CH_2 + CO$.[75] The solid line is the singlet rate constant from the measured total rates[88] and branching ratios.[87] The filled triangles are variational RRKM singlet rate constants.[70] The open circles are a more recent variational RRKM calculation based on an *ab initio* PES.[89] The filled circles are the PST rate constant for formation of the lowest *ortho* rotational state of $^1CH_2$ divided by the observed fractional population of that state. The dashed line is phase space theory.

structure shows peaks separated by some 80 cm^{-1} with rates decreasing by as much as a factor of 2.3 for an energy increase of less than 20 cm^{-1}. Even the finest structures apparent in Figure 5 are completely reproducible.

This is the first example of such peaks in a rate constant. These peaks may be understood in terms of tunneling through a barrier with a minimum at the midpoint along the reaction coordinate (Figure 4).[82,84,86] Quasi-stable resonances or vibrational levels exist inside the well for motion along the reaction coordinate. The tunneling rate is greatly enhanced at the energies of these resonances. Resonances can also be expected above the top of the barrier since the reaction coordinate changes from mostly O atom motion in the central region of the barrier to mostly H atom motion at the transition states. At the energies of these resonances, motion along the reaction coordinate tends to be reflected at transitions between H motion and O motion. *Ab initio* calculations have established that there is a broad well at the top of the barrier which is about 2000 cm^{-1} deep.[84] Quantum dynamical calculations in which the coordinates most closely coupled with the reaction coordinate are treated together in the region of the barrier reproduce the qualitative features of the observed rate data.[86] The structures in Figure 5 serve as a dramatic reminder that quantum mechanical resonances in the motion along the reaction coordinate and couplings between the reaction coordinate and other coordinates can be responsible for dramatic deviations from the classical motion along the reaction coordinate which is assumed in deriving eq 1.

Reactions without Barriers: From Completely Loose to Tightly Constrained Transition States. The recombination of two free radicals is the largest class of reactions without a barrier. Other molecules such $^1CH_2 + CO$ (Figure 4) are also sufficiently reactive to recombine without a barrier. Thus, $^1CH_2$ is formed precisely at the threshold for dissociation of the ground electronic state of ketene, 30 116 cm^{-1}.[73,74] The reaction competes with dissociation to $^3CH_2$, and so the yield of product, photofragment excitation (PHOFEX) spectrum in Figure 6, is directly proportional to the rate constant.[69,73,74,87] In the first few cm^{-1} there is only one state of singlet methylene energetically possible for each nuclear spin state (ortho and para states of the two H nuclei are conserved throughout the dissociation process).[73,74] Thus, the curve in Figure 6 is rigorously proportional to the rate constant for the first 20 cm^{-1}. The PST calculation and the experiment are in precise agreement even to the summation over the thermally populated rotational states of ground state ketene at 4 K in the jet. Thus, the positions of the steps in $W(E,J)$ are exceptionally clear and within a fraction of a cm^{-1} of the energy levels of the isolated product fragments. This is undoubtedly the sharpest spectrum showing the location of the energy levels of a transition state. More significantly, this provides a well-resolved example of the limiting case of a completely loose transition state and the opportunity to study the transition from loose to tight as energy increases.

PST rates for the completely loose transition state are compared with the observed rates in Figure 7. The transition state begins to tighten in the range between 50 and 100 cm^{-1} above threshold.[75,87] The variational RRKM theory reproduces the experimental rate.[70,88] Product vibrational state populations are predicted accurately when $W(E,J)$ for vibrationally excited products is calculated for motion on the vibrationally adiabatic potential curves leading to each vibrationally excited product state.[70,89] This results in populations of vibrationally excited states which are much larger than predicted by PST because the transition state on a surface leading to vibrationally excited products is looser than that for ground state products. The product energy state distributions have been studied and found to be accurately given by PST up to 200 cm^{-1}.[75] As energy increases, the rotational energy of $^1CH_2$ increases much less rapidly than predicted by PST. Up to an energy of 200 cm^{-1} the dynamics between the modestly tightened transition state and the separated products give fully randomized product

rotational energy state distributions. At higher energies the dynamics must become significantly adiabatic so that the product state distributions reflect to some extent the motions and energy levels at the transition state. However, this adiabaticity must be far from rigorous as each product energy state is observed precisely at its asymptotic energetic threshold.[73−75] Transitions from one adiabatic channel to another must occur quite frequently as the molecule evolves from the transition state to separated products. Such nonadiabatic dynamics may be induced by coupling with motion along the reaction coordinate, translation ↔ rotation−vibration energy transfer. It may also result from dynamics which hop between adiabats at narrowly avoided crossings.[90,91] Quantitative models for this energy flow are currently being developed.

Rate constant and product vibrational energy state distributions[92] for NCNO → CN + NO are controlled by dynamics which are qualitatively the same as described above for ketene dissociating to $^1CH_2$ + CO. However, the fragment rotational distributions are accurately modeled by phase space theory up to at least 1800 cm^{-1} above the threshold.[93]

The dissociation of NO_2 to NO + O is currently providing a wealth of information on the dynamics of reactions without a barrier.[64,77,94−101] The structure in the PHOFEX spectrum of NO_2 just above the reaction threshold is dominated by the features in the absorption spectrum. The widths of the overlapping resonances[77,94,101] have been analyzed, and a dissociation rate constant has been obtained. The opening of the channel for the first excited rotational state of NO approximately doubles the rate. The absolute rate at threshold, $(1-2) \times 10^{10}$ s^{-1}, agrees reasonably with PST when the density of states is taken from the fluorescence excitation spectrum just below threshold.[77,94,95,101] An *ab initio* calculation[64] gives the energy maximum at infinity for the first and second channels and at 3.2 Å and less for the third and higher channels (Figure 2). That is to say that within the first 10 cm^{-1} above threshold the transition state tightens dramatically.

Measurements of the rate constants for NO_2 dissociation[96,97] on the picosecond time scale and with energy resolution of 25 or 50 cm^{-1} (Figure 8) give much faster rate constants near threshold, 1.6×10^{11} s^{-1}, than those derived from the spectroscopic measurements. The data show steps with a spacing of about 100 cm^{-1} and a height comparable to the near-threshold rate. While the energy spacings are somewhat larger than those of the channel maxima predicted in Figure 2, they are certainly suggestive of the spacings between bending levels of a variational transition state as it tightens. The increase in threshold rate constant between the line width and the picosecond data is a factor of about 10. This suggests that perhaps the density of states for molecular motions inside the transition state decreases by something like an order of magnitude from the completely loose to the tight transition state. The tight transition state step height corresponds to the density of vibrational levels obtained spectroscopically near 16 000 cm^{-1} and extrapolated to the threshold near 25 000 cm^{-1} while that for the loose transition state is about an order of magnitude larger.[95] Highly anharmonic, large-amplitude motions and coupling to the many electronically excited states which approach in energy as the bond breaks may cause this large density of states for the very loose transition state. Alternatively the apparent steps in the picosecond data may not correspond to unit steps in $W(E,J)$ of height $1/h\rho(E,J)$. The observed level densities may result from the weakening of bending force constants as bonds begin to break.[102] The linewidth and picosecond data may both be fit[101] (Figure 8) with a monotonically increasing $\rho(E,J)$ and an assumed potential which tightens less rapidly than in Figure 2.

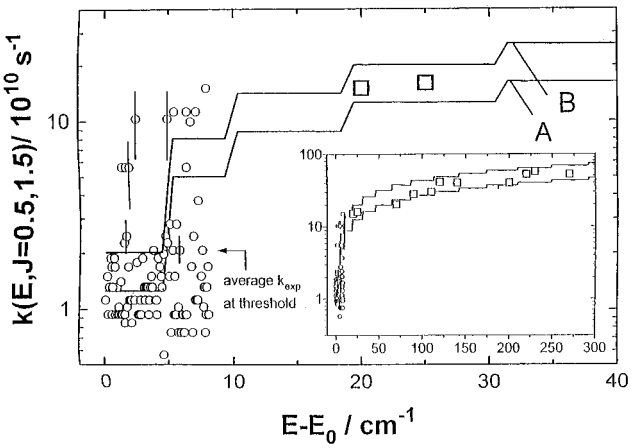

Figure 8. Experimental rate constants (○)[77,101] close to the dissociation threshold for $J = 0.5$, 1.5, experimental rate constants $k(E)$ from time-resolved picosecond experiments (open squares),[97] and SACM model calculations for $J = (0.5 + 1.5)/2 = 1$ (marked with A and B). B: SACM model calculations of specific rate constants $k(E,J)$ for $J = (0.5 + 1.5)/2 = 1$ with a calculated density of states $\rho(E,J)$ (and a calculated energy dependence), as a function of excess energy $E - E_0$. A: SACM model calculation of specific rate constants $\rho(E,J)$ for $J = (0.5 + 1.5)/2$ with an experimental threshold density of states $\rho(E,J)$[77,94,95] (with a calculated energy dependence as in B), as a function of the excess energy $E - E_0$. The box in the picture shows rate constants from the frequency[77,101] and time domain[97] and the calculations A and B on a larger energy scale (similar axis units). Reproduced with permission from ref 101. Copyright 1996 Royal Society of Chemistry.

The energy dependence of product state distributions promises to provide detailed insight into the dynamics of energy flow during product separation and into the importance of the wave function of the initial molecular eigenstate or superposition of eigenstates in determining the final products.[98−100] These experiments on NO_2 suggest that there is much left to be learned before a quantitative dynamical theory for reactions without barriers is at hand.

Quantum Statistical Fluctuations. From eq 1 it follows that the product of level density and line width for the levels of a molecule above the threshold for dissociation is $W(E,J)/2\pi$. Thus, reasonably resolved spectra of dissociating molecules can be expected for energies where only a few channels are open at the transition state.[103] For the reaction $D_2CO \rightarrow D_2 + CO$, over 1000 dissociative levels have been resolved in the Stark level-crossing spectrum of D_2CO.[76] Within an energy range of several cm^{-1} the line widths and hence the rate constants for dissociation were found to vary by over 2 orders of magnitude. The average rate agreed well with that predicted from the *ab initio* properties of the transition state. The distribution of rate constants was modeled quantitatively by assuming that the individual molecular vibrational energy levels are completely ergodic (i.e., that vibrational coupling is strong and that the wave functions of the individual levels are random linear combinations of all the functions of comparable energy in a separable basis).[104,105] These fluctuations have also been observed for the dissociation of CH_3O[106] and of NO_2.[77,94,101] The density of states is directly measured in these examples, and so eq 1 is verified completely quantitatively.

The HO_2 molecule is sufficiently small that notwithstanding its high barrier to dissociation to H + O_2 it has been possible to compute all of its vibrational energy levels up through the dissociation limit.[107] These calculations yield vibrational wave functions which appear ergodic and line widths above threshold which fluctuate just as do those observed for D_2CO, CH_3O, and NO_2. The large changes in rate constant from state to state within a narrow energy range are the quantum statistical

fluctuations expected in the quantum-state-resolved limit of the RRKM theory. The dissociation rate clearly depends strongly on the detailed vibrational wave function, and thus in some sense the chemistry is state specific; however, the molecule is behaving exactly as predicted with the statistical transition state theory.

Slow Intramolecular Vibrational Redistribution (IVR) and Mode-Selective Reaction. The dream of energizing single chemical bonds or vibrational modes so as to cause reaction at or near the locus of excitation has inspired much work over the past few decades. Under what circumstances can one expect energy transfer throughout a molecule to be slower than chemical reaction? Chemical activation studies suggest that the energy in a newly formed bond requires a time on the order of a picosecond to spread among the modes of modest-sized polyatomics.[79] The phenomena of infrared multiphoton excitation (IRMPE) and dissociation (IRMPD) were discovered in the mid-1970s.[108,109] Since sufficient energy to dissociate a molecule could be feed in through a single vibrational mode on a time scale of nanoseconds, many studies were carried out searching for mode-selective reaction processes. Isotopic selectivity based on the shifts of vibrational frequencies was soon established. However, it became clear that experimental observations could all be modeled by assuming that for energies above a few thousand cm^{-1} the nanosecond time scale for IR excitation and subsequent dissociation is long compared to the time scale for transferring energy from the pumped mode to all other modes.[110] A recent series of elegant experiments[111] with carefully controlled laser pulses have provided detailed and truly quantitative tests of this model for reactions such as $CF_3I + nh\nu_{IR} \rightarrow CF_3 + I$ with Doppler-resolved velocity profiles for individual hyperfine states of the I atom product. As pico- and femtosecond pulses become available for IRMPD, the goal of mode selectivity may become attainable.

In the past decade spectroscopic and theoretical studies[51,112] of the dynamics of IVR have progressed rapidly. This work is discussed in depth elsewhere in this special issue.[113] The results suggest that for small molecules at relatively low excitation energies IVR can be slow or incomplete. Thus, the rate of dissociation of HCO, with its barrier to H + CO formation only 7300 cm^{-1} above its vibrational zero-point energy, is not at all statistical.[114] The wave functions of vibrational levels are much better approximated as rigid-rotor-harmonic-oscillator states than as ergodic ones.[115,116] The observed dissociation rates and product energy state distributions depend very strongly and systematically on the vibrational quantum numbers of the CH stretch, CO stretch and bending vibrations.[114] The dissociation of HFCO to HF + CO with a barrier of about 16 000 cm^{-1} is an intermediate case.[117] Levels with high excitation in the out-of-plane bending vibration are weakly coupled to other vibrations.[78] IVR limits the rate of dissociation of these levels. The observed rates appear to be controlled by Coriolis coupling as they increase dramatically with rotational excitation, by as much as 10^2 for J increasing from 0 to 4.[117] Rates for molecules in $J = 0$ demonstrate the conservation of vibrational symmetry as the molecule passes through the transition state. Molecules in energy levels with an odd number of quanta of out-of-plane bend (A″ in C_s) must carry at least one of these quanta (~800 cm^{-1}) through the transition state region. Those with an even number of quanta (A′) can have all of their energy in the reaction coordinate. Thus, A″ $J = 0$ states dissociate at a rate comparable to an A′ state with ~800 cm^{-1} less energy. This effect was originally predicted for the formaldehyde molecule[118] but was not observed because no measurements were possible for $J = 0$. For $J > 0$ Coriolis mixing breaks the symmetry.

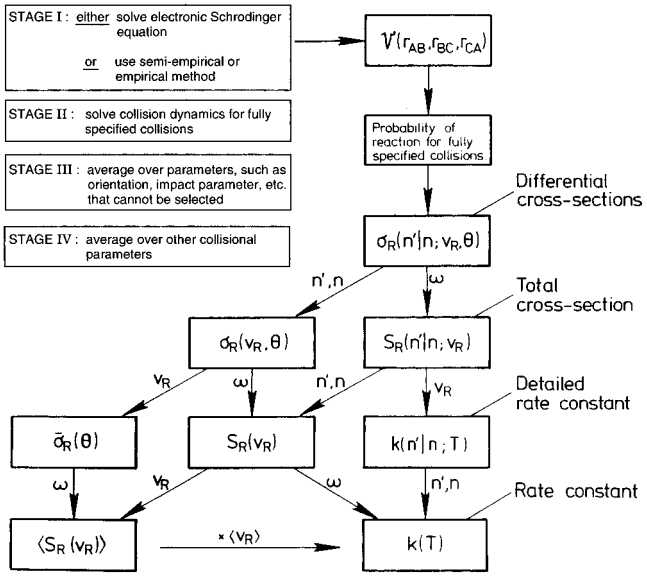

Figure 9. Flow diagram showing the connections between the potential energy surface and various parameters used to describe the results of reactions on the dynamics of bimolecular reactions at different levels of detail. The presence of a symbol close to one of the lines connecting two boxes indicates averaging over that parameter. Reproduced with permission from ref 3. Copyright 1980 Butterworths.

Notwithstanding these interesting examples, it is clear that the assumption of rapid vibrational energy randomization on which the statistical transition state theory is based is amazingly robust. The large bath of states to which vibrational relaxations occur in condensed phase[119,120] or in large molecules[121] quenches statistical unimolecular reactions. Attempts[122,123] to find underlying mode or site-specific reactions have revealed quantum yields on the order of 10^{-5}. The prospects for state-selective chemistry appear much more promising in the direct dissociations which occur following electronic excitation to repulsive potential energy surfaces.[36]

Bimolecular Reactions

The study of *bimolecular* reactions has been at the heart of efforts to understand molecular reaction dynamics since the field started to emerge as a separate discipline. Whereas *unimolecular* dynamics are largely determined by scattering from an initial state in which all the atoms are close together and are held in a more or less well-defined geometry, bimolecular reactions occur in *molecular collisions*, in which the reagents approach from large separations. In principle, the form and influence of the PES far from the minimum-energy path can be examined, but in practice, the lack of control over the impact parameters and orientations in collisions means that averaging over these quantities degrades the quality of the dynamical information that can be obtained. In attempts to circumvent this problem, ingenious efforts have been made to restrict the orientations of reagents for bimolecular reagents using directional electric fields provided externally[124] or via an excitation laser[125] or by initiating such reactions in loosely held van der Waals dimers.[126,127] The connection between the potential energy surface for a reaction and the results of experiments, with scattering calculations of one kind or another (i.e., classical or quantum mechanics)[55] providing the link, can be represented by the flow diagram shown in Figure 9.[3] Because the "natural" direction of flow is as shown, theory is subjected to the most rigorous tests by experimental observables, such as state-specific differential cross sections, which are subject to the least averaging.

The first great flowering of molecular reaction dynamics came[128] as molecular beams were brought out of the physicist's laboratory and the study of *reactive scattering* was started; i.e., the velocity (speed and angle) distributions of the products of a range of bimolecular reactions were measured. The crucial distinction was made between *direct* reactions, leading to highly nonisotropic angular distributions and generally highly specific energy disposal, and reactions proceeding via *collision complexes*, where the angular distribution, though still anisotropic, was symmetrical about $\theta = 90°$ (where θ is the scattering angle in the center-of-mass system) and the energy disposal was more statistical. At the same time, spectroscopic techniques, especially infrared chemiluminescence,[129] began to provide the distributions of product molecules over internal rovibrational states.

As described in the Introduction, these experimental advances were paralleled by a great increase in computing power enabling the results of molecular collisions to be calculated for the first time, albeit via the equations of classical mechanics. Such quasiclassical trajectory (QCT) calculations established the connection between general features of PESs and dynamical attributes of reactions.[25] However, something that was not possible in the 1960s was the accurate calculation of PESs via *ab initio* quantum chemistry, even for H_3, nor was it possible at that time to test the accuracy of QCT calculations by comparing them with the results of exact quantum mechanical (QM) scattering calculations. The ability to perform such calculations is one of several recent developments which have arguably brought molecular reaction dynamics into a second golden age.

There have been other, immensely impressive, developments in the laboratory. Until the late 1970s, reactive scattering experiments, employing supersonic expansions to produce intense beams and defined collision energies and mass spectrometers to detect scattered reaction products, occupied a commanding position in laboratory studies. They continue to provide important data, but it is photochemical and spectroscopic applications of lasers which are now revolutionizing the study of bimolecular reaction dynamics, enabling data of increasing sophistication to be gathered. Conventional mass spectrometry identifies chemical species by their mass but provides no information about the populations in molecular eigenstates. The use of tunable lasers, separate from or in conjunction with mass detection, can provide detailed information at the state-resolved level via a variety of spectroscopies (see earlier).[32] Furthermore, the use of lasers is not confined to the observation of reaction products. The power, monochromaticity, tunability, and polarization of laser sources can also be used to generate reagents in defined states or photofragments with defined translational velocities. The ingenious application of lasers has enabled experimentalists to probe a small number of reactions in exquisite detail. At least for isotopic variants of the $H + H_2$ reaction, the dream of observing state-to-state differential reaction cross sections has been fulfilled.[130,131]

A second development over the past decade, and one which can confidently be predicted to continue, is the extension of experimental and theoretical efforts of high quality to ever more complex systems. Here "complexity" has two connotations. During much of the period since 1960, our perceptions have been shaped by studies of direct reactions of the type $A + BC \rightarrow AB + C$, where A, B, and C represent atoms, and there is no minimum on the minimum-energy path across the PES leading from reagents to products. Now studies are extending to reactions involving more atoms and to reactions which occur on PESs with wells and hollows which are therefore predisposed

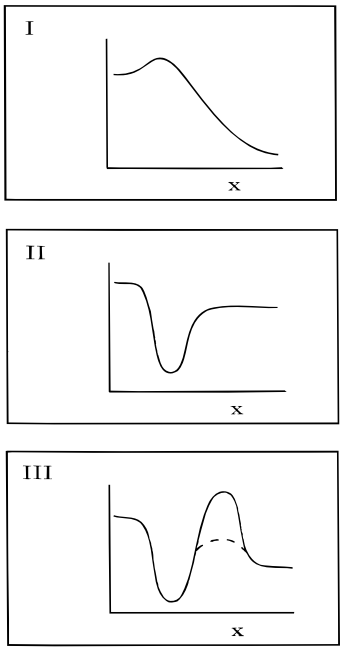

Figure 10. *Ab initio* profiles along the minimum-energy path for reactions over different types of potential energy surface.

to occur by way of collision complexes. For the moment, both calculations and experiments on such systems appear primitive when compared with those on the prototypes of direct $A + BC$ reactions:

$$H/D + H_2/D_2 \rightarrow H_2/HD/D_2 + H/D; \quad \Delta_r H_0^\circ = 0 \text{ kJ mol}^{-1} \tag{2}$$

$$F + H_2/HD/D_2 \rightarrow HF/DF + H/D; \quad \Delta_r H_0^\circ = -133.7_5 \text{ kJ mol}^{-1} \tag{3}$$

but this position can confidently be expected to change. (In eqs 2 and 3 and elsewhere, the values of $\Delta_r H_0^\circ$ refer to the fully hydrogenated reaction.)

In the remainder of this section, our present understanding of bimolecular reaction dynamics is reviewed in three subsections divided according to the broad nature of the PES which is known, or supposed, to control the dynamics. This distinction is represented in Figure 10 which displays schematic profiles of potential energy along the minimum paths leading from reagents to products. In case I, there is no minimum; this is the usual situation for reactions between (atomic or molecular) free radicals and saturated molecules, like (2) and (3), and it generally leads to direct dynamics. For case II, there is a deep well or minimum but no maximum of potential energy in either the entrance or exit channel. Such surfaces are characteristic of reactions between free radicals, such as those (in the exothermic direction) between N or O atoms and OH radicals,

$$N + OH \rightarrow NO + H; \quad \Delta_r H_0^\circ = -203._4 \text{ kJ mol}^{-1} \tag{4}$$

$$O + OH \rightarrow O_2 + H; \quad \Delta_r H_0^\circ = -69._1 \text{ kJ mol}^{-1} \tag{5}$$

in the situation where the transient complex formed contains a bond weaker than that formed when the reagents come together. The case III potential also displays a deep minimum. However, now there is a well-developed maximum in the minimum-energy path leading to the products. The height of this barrier, relative to the energy of the separated reagents, is likely to have a strong influence on the dynamics in such systems. Examples of

reactions proceeding over such surfaces include a number of those between radicals and unsaturated molecules; that between OH + CO is a well-studied example:

$$OH + CO \rightarrow CO_2 + H; \quad \Delta_r H_0^\circ = -101._7 \text{ kJ mol}^{-1} \quad (6)$$

It is important to emphasize that the relationship between the dynamics of a reaction and its PES is not necessarily simple. Even for reactions over surfaces of type I, there are questions as to how the dynamics depends on the collision energy. As the collision energy is increased, the particles become less sensitive to details of the PES and kinematic factors become more important. In addition, it may become necessary to question whether the assumption of motion across a single PES, without the influence of higher surfaces, remains valid.

For collisions over surfaces of types II and III our dynamical insights are less soundly based. There are no general rules of the type which guide us to predict energy disposal or energy requirements for direct A + BC reactions.[25] The factors which determine whether or not a reaction of type II or III proceeds via a "true" collision complex (or indeed exactly what that term means) are not well-established. The dynamics of such reactions may indeed involve direct and statistical parts, but how the formation of a collision complex and hence the importance of a statistical regime depend on the potential well depth, the exothermicity (in case II), or exit barrier height (in case III) and on the energies of the reagents would appear to be fertile ground for new experiments and for new theoretical models and calculations.

Reactions over Case I Potentials. It has been realized for a long time that the systems involving three H/D atoms offered the best chance of obtaining a complete understanding of the dynamics of any bimolecular reaction. The small numbers of atoms and of electrons simplify the *ab initio* calculations that are required to determine an accurate PES, and the light masses of the nuclei reduce the number of internal states or channels that must be included in scattering calculations. What appeared to be a definitive PES for H_3 was provided by *ab initio* calculations in the late 1970s.[132−134] These data were fitted to yield the celebrated LSTH surface[135,136] which has been used in most scattering calculations on the H_3 reactions since that time.

Unfortunately, the H_3 reactions were very difficult to study experimentally in the pre-laser days of the 1960s and 1970s, not least because the barrier to the reaction is[132−134] 40.5 ± 0.5 kJ mol^{-1}. Early crossed beam experiments using thermal sources[137] to generate the required collision energies were only able to show that the HD product from D + H_2 was backward scattered, because the collision velocities were poorly defined and the HD product states could not be measured.

For a time, the F + H_2 reaction became the prototype for bimolecular reaction dynamics. As it has only a small activation energy, is strongly exothermic, and produces a vibrationally excited product (HF) which is ideal for observation by infrared chemiluminescence, its product rovibrational distribution was one of the first to be characterized.[138,139] In addition, because a beam of F atoms is relatively easy to produce, crossed molecular beam experiments on F + D_2 were performed.[140] Because DF vibrational levels are widely spaced and there is relatively low rotational excitation, different parts of the product velocity distribution could be assigned to DF in different v' states. On the other hand, to this day, there has been virtually no work using lasers to generate reagents or detect products selectively, and the position of dynamics standard-bearer has reverted to the H_3 system.

In most modern experiments on reactions of H or D atoms, they are generated with high, defined translational velocity from the photodissociation of HX, DX (X = I, Br). Momentum conservation ensures that nearly all the recoil energy is deposited in the light H/D atom. A potential complication is that the halogen atom X may be formed in its ($^2P_{1/2}$) excited or ($^2P_{3/2}$) ground state leading to H atoms which have two different translational energies, but uncertainties can be avoided either by observing only those product states that can be accessed in the higher energy collisions or by spatially resolving the two groups of H/D atoms by making use of the fact that the transition moments leading to H + X($^2P_{3/2}$) and H + X*($^2P_{1/2}$) are orthogonal. In principle, the energies of the H/D atoms can be varied continuously, since the HX/DX spectra are broad and photolysis could be effected by tunable lasers.

The uses of lasers to prepare reagents in specific states, to detect their rates of loss, and to observe the rates of formation and internal state distributions of products are similar in that they require one (or more) tunable laser(s) to provide radiation that is in resonance with the transition energy between molecular eigenstates. In the case of detection, methods are based on absorption (e.g., absorption of infrared diode lasers), the generation of "new" photons (e.g., LIF and CARS spectroscopy), or the creation of ions (e.g., REMPI and time-of-flight ion imaging).[32] All of these techniques can provide information about translational velocities by observing the Doppler "profile" of the observed transition or by introducing delays between the pump-and-probe lasers and measuring the spatial distribution of products by a time-of-flight method.

"Traditional" reactive scattering experiments arguably reached their apotheosis with a study[141] of the D + H_2 reaction in which D atoms were generated by photolysis of DI at 248 nm and extensive scattering measurements were made at two collision energies, 51 and 97.5 kJ mol^{-1}. The resolution was sufficient to resolve individual vibrational states of the HD, which was scattered predominantly backward (relative to the initial D atom beam) but to wider angles at the higher collision energy. Comparison with quantum scattering calculations[142,143] gave good general agreement but revealed some detailed discrepancies.

A crossed beam experiment on the H + D_2 reaction employing a quite different detection method has been reported very recently.[130] A beam of H atoms was generated via laser photolysis of HI, but now the results of reactive collisions with D_2 were observed by Rydberg atom TOF spectroscopy. The product D atoms were "tagged" by exciting them to a high Rydberg state, and then they were field ionized at the entrance to a rotatable mass spectrometer. The energy resolution was 0.5%, so the D atom signals could be associated clearly with HD in different rovibrational states. Comparison of the results with QM and QCT scattering calculations revealed better but not perfect agreement with the former.

A comprehensive set of experiments on the D + H_2 and H + D_2 reactions has been performed.[131,144−148] Once again, D or H atoms were created with defined translational energy, and either the product atoms or HD($v'j'$) products were observed using reaction product imaging[148] or, in most cases, REMPI spectroscopy. The earliest experiments in this series were almost contemporary with similar experiments[149,150] which employed CARS spectroscopy to observe HD and determine the product state distributions. The comparison of the results from the two laboratories led to a lively controversy, which is now resolved: in agreement with theoretical calculations,[142,143] the integral cross sections for production of HD in specific rovibrational states vary smoothly and display no effects due

to quantum mechanical resonances. The results of these experiments at high collision energy confirm, what has long been suspected, that this reaction is predominantly adiabatic in respect of reagent and product vibrations. Thus, for D + H_2-(v=0,j) at E_{coll} = 75 kJ mol^{-1} (0.78 eV), the product vibrational populations are in the ratios HD(v'=0):HD(v'=1):HD(v'=2) = 0.83:0.15:0.02, while fractional populations change to 0.32:0.52:0.14 for D + H_2(v=1,j).

Remarkably, the reaction product imaging experiments[148] and those in which HD reaction products are observed via delayed pulsed field ionization[131] yield state-to-state differential reaction cross sections, although the experiments are now quite different from conventional crossed beam experiments. The results provide the most rigorous test yet of QM and QCT scattering calculations on a chemical reaction. The comparison reveals the superiority of the former, although the ability of QCT calculations to reproduce the experimental results to the degree which they do is quite remarkable.

Even the QM scattering results deviate from the experimental data at collision energies ≥100 kJ mol^{-1} (1 eV), a discrepancy attributed to small flaws in the PES. Given that these high-energy collisions explore regions of the surface far from the saddle point, which is where most effort has been expended in *ab initio* calculations, this observation is not too surprising. A shortcoming of the photolytic technique for generating H, D atoms is that it is difficult to apply at energies close to the reaction threshold, where any difference between classical and quantum scattering calculations might be greatest.

For some time, there appeared to be a large difference between experiment and theory in respect of the thermal rate of reaction between D atoms and H_2(v=1). Recent calculations[151] using the LSTH surface have produced a rate constant in essentially exact agreement with the most directly determined experimental value: 1.9×10^{-13} cm^3 molecule^{-1} s^{-1}.[152,153] The observed enhancement of very close to 10^3 on promoting H_2 from $v = 0$ to $v = 1$ is quite close to the prediction of vibrationally adiabatic transition state theory.[154,155]

The close agreement between theory and experiment for the H_3 system represents a real triumph for chemical physics. Some refinements still need to be made, and one very interesting problem still requires resolution (see below). Moreover one should not view this agreement—on the simplest of all chemical reactions—as the "beginning of the end" in reaction dynamics but rather "the end of the beginning". The rest of chemistry, or at least that concerned with reactions, now beckons.

As well as refinements to the PES, there have been recent theoretical calculations[156] which, at least under fairly extreme circumstances, cast doubts on the usual assumption that the H + H_2 reaction occurs over a single PES. The existence of a "geometric phase effect" at energies sufficient for the trajectories to approach a conical intersection between the surfaces associated with the lowest and first excited states of H_3 is predicted.[29] Experiments on the H + H_2 reaction at energies as high as 240 kJ mol^{-1} (2.5 eV)[12] show some of the effects indicated in the calculations.[156]

Rather surprisingly, there have been no photochemical/spectroscopic experiments on the reactions of F atoms with H_2, HD, and D_2 since the 1970s. Remarkable crossed beam experiments[157,158] have yielded definitive information on the F + H_2, HD, D_2 reactions. The resolution was sufficient to identify the scattering associated with products in different vibrational levels. For all three reactions, product scattering was predominantly backward, but sharp differences were observed for different HF/DF(v'). For example, from F + H_2, HF(v'<3) was scattered overwhelmingly in the backward hemisphere, but HF(v'=3) was scattered over a wide range of angles with a prominent forward peak. The results were not well-matched by QCT calculations, and the conclusion was reached that the PES was inadequate.

The provision of an accurate PES for FH_2 has been a long-standing problem. Although a large number of QCT calculations have reproduced the product state distributions from F + H_2 quite well, the surfaces have been known to be flawed, in that the calculations failed to reproduce the thermal rate constant and its dependence on temperature. The accuracy of the *ab initio* surfaces for some reactions can now be tested by observing the photoelectron spectrum of the negative ion of the system.[159] FH_2^- is promoted to regions on the neutral PES close to the transition state for F + H_2 → HF + H, and the photoelectron spectrum shows considerable structure. Recently, these experimental results[159] have been used[160] to test a new generation of PESs for FH_2. Impressive agreement was found between the experimental results and those of QM scattering calculations on a surface based on a "benchmark" full CI calculation.[161] An important point was that the *ab initio* calculations had suggested that the (albeit shallow) minimum on the neutral FH_2 surface was associated with a bent geometry so that the photoelectron spectrum showed structure associated with the excitation of this mode.

The comparison between theory and experiment for the FH_2^- spectrum might suggest that our understanding of the F + H_2 reaction is close to that achieved for the H_3 system. However, comparisons of theoretical[162] state-specific integral and differential cross sections for F + H_2 with those from the beam experiments[157,158] suggest that this conclusion might be premature. The overall agreement between experiment and theory is satisfactory but incomplete. In particular, the extent of forward scattering is greater than is seen either in the experiments or in QCT calculations. The difference between QCT and QM calculations in regard to forward scattering is attributed to the inability of the classical trajectories of high orbital angular momentum to tunnel through barriers arising from the combined effect of potential energy and centrifugal forces. It is concluded[162] that quantum effects are vital in this reaction and that, to account for discrepanices in the extent of forward scattering, the PES may need further refinement, perhaps via the inclusion of spin−orbit effects which are likely to give a slightly high barrier.

The H + H_2 and F + H_2 reactions provide examples of the kinematic combinations often referred to as (light + light-light) and (heavy + light-light).[25] Recent experiments, again using photodissociation to generate fast reagent atoms, have explored some aspects of the dynamics of the (light + light−heavy) and (heavy + light−heavy) systems. Using CARS spectroscopy, the H_2 formed in the reactions

$$\mathrm{H + RH\ (RH = HCl, HBr, HI, CH_4, C_2H_6, C_3H_8, CDCl_3)} \rightarrow \mathrm{H_2 + R}$$

$$\Delta_r H_0^\circ = -4.3, -69.5, -137.4, -0.2, -25, -25, -36\ \mathrm{kJ\ mol^{-1}} \quad (7)$$

at a collision energy of 1.3 eV has been observed.[163−166] The H_2 internal energy yield is ≤20% of the total energy available in all cases, consistent, at least for the thermoneutral or almost thermoneutral reactions, with notions of vibrational adiabaticity[154,155] and, more generally, with the idea of excess translational energy in the reagents being largely retained as translational energy in the products.[131] For the reactions with the hydrogen halides, the experiments have been supported by QCT

calculations[167] which are able to reproduce the observations quite well, although for H + HI there is a significant difference in the product vibrational distributions, with the calculations suggesting a monotonic decrease in the populations with v', whereas the experimental distribution peaks at $v' = 1$.

The application of sophisticated, largely laser-based, experimental methods has provided unprecedented dynamical detail for some three-atom direct reactions, notably H + H_2 and F + H_2 and their isotopic variants. One can confidently expect the increasing application of such methods to reactions involving more atoms. This progression allows one to address new questions, especially those relating to vibrational selectivity and specificity. For example, in a reaction such as A + BCD → AB + CD, how does the rate or cross section depend on excitation in the BCD vibrations and how is energy partitioned between the modes of the AB and CD products? Clearly, similar questions can be posed for reactions of the reverse type; i.e., AB + CD → ABC + D. Among other factors, the answers will depend on the thermochemistry: whether the reaction is exothermic, thermoneutral, or endothermic. Experiments on the influence of vibrational excitation on endothermic reactions like A + BCD → AB + CD and the interpretation of the results are described elsewhere in this issue.[168] Our discussion is limited to exothermic reactions.

The experiments which have been performed on such systems are primitive compared with those on reactions such as D + H_2 and H + D_2, since there are several fundamental difficulties associated with transferring the techniques used to study D + H_2 to more complex reactions of the AB + CD → ABC + D type. These are largely not present for experiments on A + BCD → AB + CD, where A, B, and C are all atoms but D can be a polyatomic moiety. Again, pulsed laser photolysis of a diatomic precursor can be used to generate monoenergetic atoms (H or Cl) in order to study the results of reactive collisions at a defined collision energy. Moreover, with a suitable choice of reaction, the product states of the diatomic product AB can be interrogated by one of the panoply of spectroscopic techniques which have already be identified in this article. The same may be true of CD, as long as it is diatomic, but otherwise it is difficult to find a method which allows identification of individual quantum states of this product.

As already reported, the dynamics of the reactions of H atoms with some alkanes and substituted alkanes have been investigated,[163−166] and the results have been compared with those for the H + HX (X = Cl, Br, I) reactions, which are kinematically similar, though not always thermochemically the same. One surprising feature of the H + HR systems, not found for H + HX, is that the H_2 product vibrational and rotational distributions are positively correlated; i.e., the rotational energy yield increases with the product vibrational quantum number. It has been tentatively suggested that the "additional" rotational excitation in $H_2(v'>0)$ may result from secondary encounters between H_2 and R, as these products start to separate. As yet, there has been no identification of the internal states of the R product.

The dynamics of reactions of energy-selected Cl atoms and hydrocarbons have been studied[169,170] by creating the atoms by pulsed laser photolysis of Cl_2 at 355 nm. Because (a) this photolysis is performed fairly close to threshold, (b) the energy is shared equally between the photolysis products, and (c) the Cl atom is the heavy partner in subsequent potentially reactive collisions, the collision energy is quite low: 15.3 kJ mol^{-1} (0.159 eV) in the case of Cl + CH_4. HCl(v',j') was detected[169,170] by (2 + 1) REMPI spectroscopy. It is interesting to note that these reactions, Cl + HR → HCl + R, are approximately thermoneutral (for R = CH_3) or mildy exothermic (for R = C_2H_5 and C_3H_7) and that they represent a third, and important, kinematic case; where an H atom is transferred between two heavy moieties (i.e., heavy + light−heavy → heavy−light + heavy).

With an experimental arrangement of two crossed uncollimated beams,[169] the collision energy is relatively poorly defined. For Cl + CH_4, HCl($v'>0$) was energetically inaccessible and the HCl($v'=0$) product was found only in low rotational states and scattered predominantly backward. The exothermicity of the reactions with R = C_2H_5 and C_3H_7 allows higher v' states to be accessed. However, both the vibrational and rotational yields remain low, prompting the suggestion[169] that reaction occurs through a transition state in which the Cl--H--C atoms are fairly tightly constrained to linearity, a conclusion similar to that reached from earlier measurements on the reactions of O(^{3}P) with hydrocarbons.[171]

Although superficially similar, the experiments performed[170] on Cl + CH_4 are rather different and provide a much greater level of detail, at least for one state-specific channel, Cl + CH_4($v=1,j=1$) → HCl($v'=1,j'$) + CH_3. Cl_2 and CH_4 were coexpanded, and the Cl_2 was photolyzed to generate Cl. The ions from HCl($v'=1,j'$) created by (2 + 1) REMPI were detected with high velocity resolution, allowing differential cross sections to be extracted for particular ($v'=1,j'$) states. Although both HCl($v'=1,j'=1$ and 3) scatter predominantly forward, the angular distributions depend on j'. One suggestion for the origin of forward scattering is that there is a vibrationally adiabatic minimum on the surface correlating with HCl($v'=1$) + CH_3 which allows the transition state to survive long enough to rotate. Classically, the minimum is associated with the "trapping" of the H atom between its two heavy associates. Quantum mechanically, this behavior is linked to a resonance which should be highly sensitive to the energy of the system.

Four-atom reactions of the type AB + CD → ABC + D are now attracting considerable attention, especially from theoreticians.[55,172,173] The prototypical reactions are

$$OH + H_2 \rightarrow H_2O + H; \quad \Delta_r H_0^\circ = -61.9 \text{ kJ mol}^{-1} \quad (8)$$

$$CN + H_2 \rightarrow HCN + H; \quad \Delta_r H_0^\circ = -53 \text{ kJ mol}^{-1} \quad (9)$$

Reaction 8 has the advantage that three of its four atoms are hydrogen, meaning that the construction of accurate potential energy surfaces by *ab initio* methods is relatively easy. On the other hand, the $X^2\Pi$ ground state of OH is split by spin−orbit coupling. In this respect, reaction 8 is not unlike that between F and H_2, and again it may be necessary to include spin−orbit effects to reproduce the ground state PES accurately. Setting aside spin−orbit effects, it will be harder to perform *ab initio* calculations on the CN + H_2 system because of the greater number of electrons, although now only a single PES correlates with the reagents, CN($^2\Sigma^+$) + H_2($^1\Sigma_g^+$), and products, HCN($^1\Sigma^+$) + H(^{2}S), in their ground states.

Scattering calculations on four-atom reactions are becoming increasingly sophisticated.[174,175] Most of those on OH + H_2 use the Schatz−Elserma surface,[176] or a modified form of it, and new *ab initio* calculations using the full power of modern methods are sorely needed. The results, as regards vibrational selectivity and specificity, largely confirm ideas based on simpler theoretical concepts, such as vibrationally adiabatic transition state theory.[154,155] For example, vibrational excitation of the "spectator" OH bond has little effect on the reaction cross sections and rate constants, whereas excitation of the H_2 vibration causes a large decrease in the translational threshold and hence a large increase in the thermal rate constant.

Rather surprisingly, there have been no recent measurements on the influence of reagent vibrational excitation on the reaction between OH and H_2. Older measurements[177−179] suggest a rate enhancement of only ca. 50% on exciting OH from $v = 0$ to $v = 1$ but a factor of ca. 100 when H_2 is promoted from $v = 0$ to $v = 1$. The finding that, in a direct reaction between a radical and a saturated molecule, excitation of the free radical's vibration causes little acceleration of the rate of reaction has been confirmed in a series of bulb experiments on reactions of OH and CN.[180−182] Recent measurements[183] on the CN + HCl → HCN + Cl reaction find a similar effect to that for OH + H_2: the rate is enhanced by about 150 times by exciting the HCl to $v = 1$ but insignificantly by a similar excitation of the CN radical. The dynamics of the reverse, endothermic, reactions to (8) and (9), in particular, the effects of selective excitation of the vibrations of either H_2O or HCN, are considered in detail elsewhere in this special issue.[168]

Reactions 8 and 9 have activation energies of 17.5 kJ mol^{-1} and 17.2 kJ mol^{-1}, respectively. Most of the limited data available at the state-specific level have been determined in bulb experiments. Although radicals such as OH and CN can be generated by pulsed photolysis of suitable precursors, the increasing number of degrees of freedom in the photolytic products means that the radicals are produced with a spread of translational energies—in contrast to the situation when H atoms are generated from HBr or HI. In some respects, this restores crossed molecular beam experiments to their position of primacy. The dynamics of the OH + D_2 reaction have been studied[184] at a collision energy of 26 kJ mol^{-1} (0.27 eV). The finding that the HOD is strongly backscattered and that the integral cross section is only 0.4 Å^2 is consistent with reaction via a rebound mechanism through a tightly constrained transition state. Thirty-two percent of the available energy is released as product translational energy, indicating appreciable internal excitation of the HOD which agrees with the results of theoretical calculations[173] and with the observation that the strongly endothermic reverse reaction is greatly accelerated by exciting localized stretching modes in H_2O or HOD.[168] As this article was being completed, the first report was received of the observation of vibrationally excited H_2O formed in reaction 8.[185] The technique used was that of infrared chemiluminescence, and the overall fractional yield of vibrational energy was estimated to be $\langle f_{v'} \rangle \approx 0.6$ with the bending mode levels populated up to the energy limit and the populations showing an inversion.

Experiments on the reverse reactions to (8) and (9) depend on the capacity to provide O−H or C−H stretching vibrations with large amounts of energy by overtone excitations of appreciable intensity. Conversely, H_2O and HCN are not easy to detect in a state-specific way using laser-based spectroscopies. Some vibrationally specific measurements on the HCN formed in the reaction between CN radicals and C_2H_6 have been performed,[186] using time-resolved absorption of infrared radiation from tunable diode lasers. Extension of this technique and the development of others for the state-specific detection of polyatomic products of reactions are badly needed and are likely to provide major advances over the next few years.

Reactions over Case II Potentials. Bimolecular exothermic reactions between two free radicals occur across case II potentials when the bond formed as the radicals approach is not the weakest bond in the combined species. (Experiments on the reverse unimolecular reactions across potentials of this kind are discussed in the previous section.) Their importance in various environments (combustion systems, the atmospheres of planets, including the Earth's, and interstellar clouds), as well as fundamental interest, has stimulated studies of the kinetics of many such reactions over the past two decades, and it is now appreciated that their rates are usually determined by mutual "capture"[187,188] of the reagents on the long-range attractive potential between them. By contrast, there have been only a few studies of the dynamics of radical−radical reactions. The experiments are hampered by the difficulty of generating sufficient radicals under sufficiently controlled conditions. These difficulties are reduced in those cases when one of the reagents is NO, NO_2, or O_2.

Reactions 4 and 5 between OH radicals and N and O atoms are examples of the simplest (three-atom) class of radical−radical reaction. The reverse of (5) is perhaps the most important reaction in combustion, and there have been numerous dynamical studies of it:[189−191] partly because translationally "hot" H atoms can be generated to overcome the endothermicity, partly because O_2 does not need to be produced *in situ*, and partly because the OH reaction product lends itself to sensitive state-specific detection via LIF spectroscopy. The reaction between NO and H atoms is too endothermic to be studied easily using hot H atoms. However, the NO product vibrational state distribution from reaction 5 has been measured,[192] and the results have been compared with those from QCT calculations.[193] Although the experimental distribution is close to the phase space distribution, it is unlikely that true collision complexes form.[192,193] The system is too small, the exothermicity is too great, and NOH/HNO potential wells[193] are too shallow for the three atoms to remain together long enough for more than a few vibrations.

Two four-atom radical−radical systems have been studied in similar detail to N + OH:

$$H + NO_2 \rightarrow OH + NO; \quad \Delta_r H_0^\circ = -123.8 \text{ kJ mol}^{-1} \qquad (10)$$

$$CN + O_2 \rightarrow NCO + O; \quad \Delta_r H_0^\circ = -56 \text{ kJ mol}^{-1} \qquad (11)$$

A spectroscopic study[194,195] has established the product vibrational state distributions of both products of reaction 10 under thermal conditions. Again, the evidence is that any formation of complexes is insufficient to allow complete energy randomization: the OH is appreciably more excited than the NO.

The reaction between CN and O_2 has been investigated in both bulb[196,197] and beam[198] experiments and is the subject of a recent review.[199] It is unusual in that it yields a linear triatomic product whose internal states can be probed via a bound−bound electronic transition—so far, LIF spectroscopy has been used exclusively. However, these studies demonstrate the difficulties involved when one makes the relatively small step from a diatomic to a triatomic product: perturbations in the spectrum are rife, making it difficult to transform LIF intensities into relative rovibronic state populations. The results derived from room temperature bulb experiments show considerable excitation of the bending mode in NCO, in contrast to those obtained in a crossed beam arrangement where the reagent rotations are cooled by supersonic expansion and most of the NCO is observed in states associated with little or no excitation of the bending vibration. This contrast suggests that reaction must proceed quite directly with little restraint to particular intermediate geometries. Consequently, the dynamics is, at least partially, adiabatic in respect of the reagent rotations which correlate with the doubly degenerate product bending vibration.

One quite unique experiment has been performed on the CN + O_2 reaction. Using rotatable beam sources to provide continuously tunable collision energies, excitation functions have

been measured[40] for the production of NCO in individual rovibronic states. This is perhaps the only example of the experimental measurement of a quantity fundamental to reaction dynamics: the integral reaction cross section and how it varies with collision energy. The measured cross section decreases with collision energy in a way which is quantitatively consistent with the negative temperature dependence of the thermal rate constant.[40,199]

Reactions over Case III Potentials. Case III potentials are characterized by both a deep well and a well-defined maximum along the minimum-energy path. One well-known example of such a system is where reaction involves association of two substituted alkyl radicals followed by the elimination of a hydrogen halide via a four-center transition state, e.g.

$$CH_3 + CF_3 \rightarrow CH_2{=}CF_2 + HF; \quad \Delta_r H_0^\circ = -303 \text{ kJ mol}^{-1} \tag{12}$$

In this case, the energy of the four-center transition state, estimated from studies of the thermal decomposition of CH_3-CF_3, is appreciably lower than the energy associated with separated reagents. At least semiquantitatively, the observed disposal is consistent with the notion that the energy possessed by the $CH_3CF_3^\dagger$ energized adduct in excess of that at the four-center transition state is shared statistically between all the degrees of freedom, consistent with conservation of angular momentum, whereas the energy released in the direct motion from this transition state to the separated products will appear in specific modes and will, to a large extent, reflect changes in the internal coordinates along this part of the minimum-energy path. Thus, the HF from reaction 11 picks up more than its democratic share of the energy released[200] because the H--F distance in the four-center transition state exceeds that in isolated HF.

Clearly, the dynamics of reactions over case III potentials depend strongly on the relative potential energies of the reagents and the barrier in the exit channel. An especially interesting case arises when these energies are similar as in reaction (6) between OH and CO. Energized HOCO complexes formed in OH + CO collisions appear to have a roughly equal chance of dissociating back to OH + CO or to CO_2 + H, and this situation is responsible, at least in part, for the unusual temperature dependence of the rate of this important reaction. Calculations[201,202] modeling the available kinetic data indicate that the zero-point energies of the transtion state leading to HOCO (TS1) and that between HOCO to CO_2 + H (TS2) are very similar, although *ab initio* calculations[203] on the surface (see Figure 11) suggest an appreciably higher barrier at TS2.

Dynamical studies of reaction (6) include a crossed beam study[184] at a collision energy of 59 kJ mol^{-1} (0.61 eV) and a measurement using kinetic infrared absorption of the distribution over vibrational states of CO_2 produced in the reaction at 298 K.[204,205] The finding of very little vibrational excitation ($f_{v'}$ = 0.06) is consistent with the results of the molecular beam experiments and confirms that the O--C--O structure in TS2 is close to that in isolated CO_2.[203] In the hyperthermal collisions of the beam experiments, 64% of the available energy is channeled into the relative motion of the CO_2 and H products.

There have been numerous elegant dynamical studies of the reverse reaction between H + CO_2.[97,206−213] Once again, the energy of translationally hot H atoms overcomes the endothermicity. Experiments, under normal bulk gas-phase conditions, have determined the integral reaction cross section[206] and the OH rovibrational distribution by LIF spectroscopy[206−208] and the CO vibrational state distribution by kinetic infrared absorption.[209] This reaction has also been initiated by photolysis of CO_2−HX (X = I, Br) van der Waals complexes.[95,210−213] The delay in appearance of the OH product is attributed to the influence of the deep HOCO well although the interpretation of the measurements is complicated by possible "trapped atom effects" due to the presence of the slowly moving X atom.

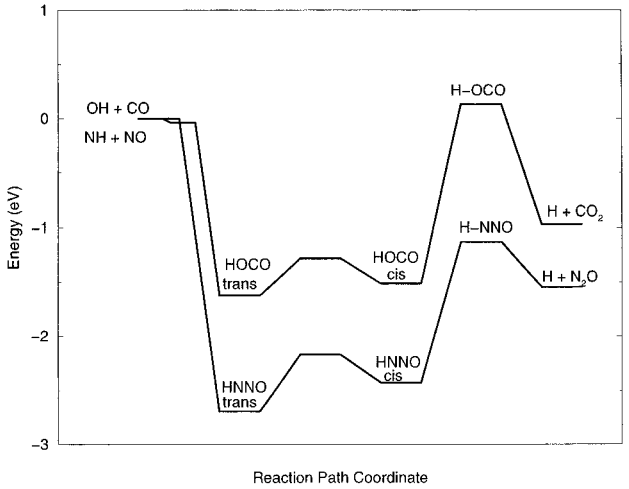

Figure 11. *Ab initio* profiles of potential energy along the reaction paths for the isoelectronic reactions: OH + CO → CO_2 + H and NH + NO → N_2O + H. Reproduced with permission from ref 173.

Although the kinetics of the OH + CO reaction now appear to be quite well-understood,[202] experimental and theoretical studies of the dynamics of this interesting and important reaction are bound to continue. One unsolved puzzle is the possible role of tunneling[202,214] through the barrier associated with TS2. The *ab initio* calculations[203] predict a barrier higher than that which is inferred[202] from modeling the rate constant data without the inclusion of tunneling.

Given the difficulty of applying the most sensitive laser spectroscopies to CO_2, and the capacity both to create H atoms of high defined velocity and to detect OH and CO by sensitive laser spectroscopies, it is likely that future detailed studies of this fascinating system will concentrate on the endothermic reaction between H and CO_2, as has proved to be the case with reaction 5. It is also interesting to note that the NH + NO system is isoelectronic with OH + CO, the reaction yielding N_2O + H is of similar exothermicity to reaction (8), and the kinematics of the reactions are also very alike.[173] Although the potentials for both reactions are of type III, that for NH + NO has a barrier which is much lower than the energy of the separated reagents[173] (see Figure 11). Consequently, a much smaller fraction of the total energy associated with the $HNNO^\dagger$ adducts will be needed in the motion along the reaction coordinate at TS2 than in the HOCO case, and a comparison of the energy partitioning and angular distributions should make an interesting and revealing comparison with the results already obtained for reaction 5. The reverse reaction between H and N_2O has been studied both in isolated binary collisons and with the reaction initiated in van der Waals complexes.[215,216] Both the relative yields of NH (+NO) and of OH (+N_2) and the OH rotational level distributions are markedly different under the two sets of conditions, whereas the NH rotational level distributions are quite similar.

Conclusion

Our understanding of the dynamics of both unimolecular and bimolecular reactions has improved immeasurably in recent years. The use of lasers with jet-cooled samples has improved the definition of energy and angular momentum in the reactant-

(s), and concomitant improvements in time resolution have resulted from the use of short laser pulses. These experimental advances have been paralleled by progress in theory.

The resolution of product quantum states has added a new dimension to unimolecular dynamics. The concept of the transition state has sharpened greatly. In the past, the geometry, barrier height, and vibrational frequencies of the transition state in RRKM theory were adjusted to fit thermal unimolecular reaction rate data. Usually these data could be described with three independent parameters, and so chemists formed a comfortable view of the transition state as a method of rationalizing data and estimating the phase space available for reaction to various products. Now we understand that the concept of quantized vibrational level thresholds at the transition state is quantitatively meaningful. There have been successful quantitative tests of the ability of *ab initio* theory to calculate transition state geometries accurately and barrier heights to a few kJ/mol for simple systems. Predicted frequencies tend to be somewhat too high for the softest modes which are of most importance in determining rates; however, the basic normal modes and sequence of frequencies seem to be correctly predicted.

For unimolecular reactions, RRKM theory can be used with *ab initio* results to predict rate constants to within a factor of 2 or 3 and may be used for quantitative extrapolation to conditions not accessible in the laboratory but important in practical situations. Experiments on single molecular eigenstates have revealed quantum statistical fluctuations in rates which are predicted quantitatively in the appropriate extension of RRKM theory. Many experiments seeking to demonstrate nonstatistical or non-RRKM dynamics have established the very wide range of applicability of the RRKM model. A few such experiments have demonstrated a lack of complete vibrational energy randomization in a reactant molecule. Dynamical theory has provided an exact quantum analog to RRKM theory which will combine with future experiments to define the extent to which quantized motion along the reaction coordinate and coupling between the reaction coordinate and vibrational degrees of freedom at the transition state are important. The future should also bring a much more complete understanding of the dynamics of energy flow as reaction products separate on a surface without a barrier to recombination.

In the realm of bimolecular reactions, progress has been no less spectacular. Because of space constraints, in this article we have emphasized how understanding has been advanced by the measurement of scalar properties, such as product state distributions and state-to-state rate coefficients with resolution at the vibrational and rovibrational level. Increasing use is now being made of the polarization of the radiation provided by laser sources to probe vector properties, especially correlations involving any preference in the rotational plane(s) of reactant and product molecules. This type of experiment that was originally developed to probe the dynamics of more-or-less direct photodissociations is now being applied to an increasing number of bimolecular reactions. As well as the experiments on reactions of H and Cl atoms that have already been described,[32,125] we refer to work on the reactions of $O(^3P)$ atoms with CS[217] and of $O(^1D)$ atoms with N_2O and CH_4.[218−220] There is little doubt that the emphasis on such experiments, especially in dynamical studies of simple bimolecular reactions, will grow.

Vibrational mode effects on bimolecular reactions, both selectivity in reagents and specificity in products, have been emphasized in the present article. The rapidity of rotational energy transfer makes it more difficult to study the effects of reagent rotations on reactivity. For direct reactions, quasiclassical trajectories indicate that there are two competing effects.[221] Rotational energy can be used to surmount potential energy barriers to reaction. On the other hand, increasing rotational excitation can destroy the preferred orientation for reaction so that molecules in high rotational states react more slowly. For the reactions of Ca and Sr atoms with HF, which only become energetically possible for HF(v=1), it has been found that there is no discernible increase in the reaction rates as HF is selectively excited to rotational levels between $J = 1$ and $J = 7$ in $v = 1$.[222,223]

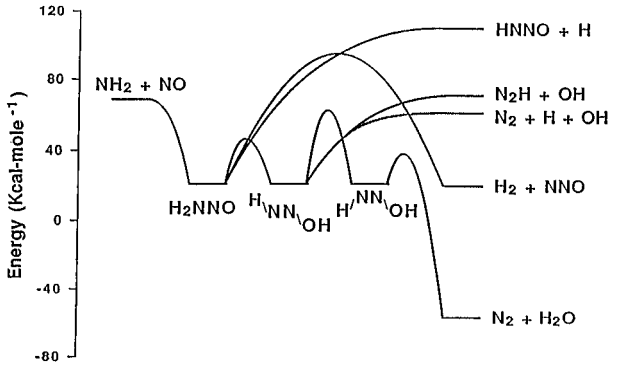

Figure 12. Profiles of potential energy along the reaction paths for the reaction between NH_2 and NO. Reproduced with permission from ref 6. Copyright 1990 Annual Reviews.

There is little doubt that experiments will increasingly emphasize the dynamics of more complex bimolecular reactions: larger species reacting over more complex potential energy surfaces. The type of PES which we have called type III is far from being the most complicated known for elementary reactions. A number are known to proceed along minimum-energy paths which can be likened to switchbacks with the presence of several bumps and hollows. One of the most remarkable is that shown in Figure 12 for the reaction

$$NH_2 + NO \rightarrow N_2 + H_2O; \quad \Delta_r H_0^\circ = -517.1 \text{ kJ mol}^{-1} \quad (13)$$

which is very important in strategies to combat the emission of nitrogen oxides from internal combustion engines. Clearly, with such a reaction, the distinction between bimolecular and unimolecular reaction dynamics becomes blurred. Although the reaction rate is determined by an initial capture mechanism leading to the formation of an energized (H_2N-NO) complex, the subsequent, rapid steps of reorganization leading eventually to the reaction products may be more usefully described by the methods applied to unimolecular reactions. We can confidently expect the dynamics of reactions as complicated as this to be investigated in the coming years, not only by measurements on the overall reaction but also by ingenious experiments on the individual microscopic steps of the reaction.

If the methods of molecular reaction dynamics are to be applied to more complex chemical systems, it seems likely that the relentless development of more and more ingenious photochemical and spectroscopic techniques will need to continue. In this respect, the investigation of molecular reaction dynamics in the gas phase will continue to serve an important mission that can be identified in its 30 years of development: namely, as the standard-bearer in the investigation of molecular phenomena lying across the traditional boundary between chemistry and physics. Many of the methods of molecular reaction dynamics, as well as the ways in which dynamicists think and ask questions, have now begun to permeate other fields: most noticeably, gas−surface phenomena[224] and processes of energy transfer and reaction in solution.[5] This interchange of techniques

and ideas is likely to continue as the field of molecular reaction dynamics continues to expand its field of view to reaction systems that are more complex than those which have been investigated in such exquisite detail toward the end of *The Journal of Physical Chemistry's* first century.

Acknowledgment. We thank our co-workers and collaborators for their contributions to the work from our laboratories. CBM's work has been supported by the National Science Foundation under Grants CHE8816552 and CHE9316640 and by the Chemical Sciences Division of the U.S. Department of Energy under Contract DE-AC03-76SF0098. IWMS's work has been supported by SERC, EPSRC, and the CEC through various programs.

References and Notes

(1) Bodenstein, M.; Lind, S. C. *Z. Physik Chem. (Munich)* **1907**, *57*, 168.
(2) Pilling, M. J.; Seakins, P. W. *Reaction Kinetics*; Oxford University Press: Oxford, 1995.
(3) Smith, I. W. M. *Kinetics and Dynamics of Elementary Gas Reactions*; Butterworths: London, 1980.
(4) Molina, M.; Hofmann, M. R. *J. Phys. Chem.* **1996**, *100*, xxx.
(5) Hochstrasser, R. M. *J. Phys. Chem.* **1996**, *100*, xxx.
(6) Miller, J. A.; Kee, R. J.; Westbook, C. J. *Annu. Rev. Phys. Chem.* **1990**, *41*, 345.
(7) Wayne, R. P. *Chemistry of Atmospheres*, 2nd ed.; Clarendon Press: Oxford, 1991.
(8) Duley, W. W.; Williams, D. A. *Interstellar Chemistry*; Academic Press: London, 1984.
(9) Herbst, E. *Annu. Rev. Phys. Chem.* **1995**, *46*, 27.
(10) Norrish, R. G. W. In *Les Prix Nobel en 1967*; The Nobel Foundation: Stockholm, 1967; p 181.
(11) *Faraday Discuss. Chem. Soc.* **1962**, *33*.
(12) *Faraday Discuss. Chem. Soc.* **1967**, *44*.
(13) *Faraday Discuss. Chem. Soc.* **1973**, *55*.
(14) London, F. *Z. Electrochem.* **1929**, *35*, 552.
(15) Hirschfelder, J.; Eyring, H.; Topley, B. *J. Chem. Phys.* **1936**, *4*, 170.
(16) Wall, F. T.; Hiller, L. A.; Mazur, J. *J. Chem. Phys.* **1958**, *29*, 255.
(17) Wall, F. T.; Hiller, L. A.; Mazur, J. *J. Chem. Phys.* **1961**, *35*, 1284.
(18) Blais, N. C.; Bunker, D. L. *J. Chem. Phys.* **1962**, *37*, 2713.
(19) Blais, N. C.; Bunker, D. L. *J. Chem. Phys.* **1963**, *39*, 315.
(20) Blais, N. C.; Bunker, D. L. *J. Chem. Phys.* **1964**, *41*, 2377.
(21) Karplus, M.; Porter, R. N.; Sharma, R. D. *J. Chem. Phys.* **1964**, *40*, 2033.
(22) Karplus, M.; Porter, R. N.; Sharma, R. D. *J. Chem. Phys.* **1965**, *43*, 3259.
(23) Polanyi, J. C.; Rosner, S. D. *J. Chem. Phys.* **1963**, *38*, 1028.
(24) Luntz, P. J.; Nemeth, E. M.; Polanyi, J. C.; Rosner, S. D. *J. Chem. Phys.* **1964**, *44*, 1168.
(25) Polanyi, J. C. *Acc. Chem. Res.* **1972**, *5*, 161.
(26) Herschbach, D. R. *Faraday Discuss. Chem. Soc.* **1962**, *33*, 149.
(27) Miller, W. B.; Safron, S. A.; Herschbach, D. R. *Faraday Discuss. Chem. Soc.* **1967**, *44*, 108.
(28) Charters, P. E.; Polanyi, J. C. *Faraday Discuss. Chem. Soc.* **1962**, *33*, 107.
(29) Anlauf, K. G.; Kuntz, P. J.; Maylotte, D. H.; Pacey, P. D.; Polanyi, J. C. *Faraday Discuss. Chem. Soc.* **1967**, *44*, 183.
(30) *Appl. Opt.* **1965**, *Suppl. 2*.
(31) *Appl. Opt.* **1971**, *10*, 1717−2010 (Special Issue on Inelastic Collisions and Nonequilibrium Processes).
(32) Houston, P. L. *J. Phys. Chem.* **1996**, *100*, 12757.
(33) Khundkar, L. R.; Zewail, A. H. *Annu. Rev. Phys. Chem.* **1990**, *41*, 15.
(34) Dantus, M.; Rosker, M. J.; Zewail, A. H. *J. Chem. Phys.* **1988**, *89*, 6128.
(35) Rose, T. S.; Rosker, M. J.; Zewail, A. H. *J. Chem. Phys.* **1989**, *91*, 7415.
(36) Butler, L. J.; Neumark, D. M. *J. Phys. Chem.* **1996**, *100*, 12801.
(37) Zewail, A. H. *J. Phys. Chem.* **1996**, *100*, 12701.
(38) Liu, K.; Hall, G.; McAuliffe, M. J.; Giese, C. F.; Gentry, W. R. *J. Chem. Phys.* **1983**, *80*, 3494.
(39) Hall, G.; Liu, K.; McAuliffe, M. J.; Giese, C. F.; Gentry, W. R. *J. Chem. Phys.* **1984**, *81*, 5577.
(40) Macdonald, R. G.; Liu, K.; Sonnenfroh, D. M.; Liu, D.-L. *Can. J. Chem.* **1994**, *72*, 660.
(41) Head-Gordon, M. *J. Phys. Chem.* **1996**, *100*, 13213.
(42) Eyring, H. *J. Chem. Phys.* **1935**, *3*, 107.
(43) Evans, M. G.; Polanyi, M. *J. Chem. Soc., Faraday Trans.* **1935**, *31*, 805.
(44) Miller, W. H. *Acc. Chem. Res.* **1976**, *9*, 306.
(45) Pollak, E. In *Theory of Chemical Reaction Dynamics*; Baer, M., Ed.; CRC Press: Boca Raton, FL, 1985; Vol. III, p 1.
(46) Truhlar, D. G.; Isaacson, A. D.; Garrett, B. C. In *Theory of Chemical Reaction Dynamics*; Baer, M., Ed.; CRC Press: Boca Raton, FL, 1985; Vol. III, p 65.
(47) Truhlar, D. G. *J. Phys. Chem.* **1996**, *100*, xxx.
(48) Marcus, R. A. *J. Phys. Chem.* **1952**, *20*, 359.
(49) Forst, W. *Theory of Unimolecular Reactions*; Academic Press: New York, 1973.
(50) Gilbert, R. G.; Smith, S. C. *Theory of Unimolecular and Recombination Reactions*; Blackwell: Oxford, 1990.
(51) Lehmann, K. K.; Scoles, G.; Pate, B. H. *Annu. Rev. Phys. Chem.* **1994**, *45*, 241.
(52) Lovejoy, E. R.; Kim, S. K.; Moore, C. B. *Science (Washington, D.C.)* **1992**, *256*, 1542.
(53) Kim, S. K.; Lovejoy, E. R.; Moore, C. B. *J. Chem. Phys.* **1995**, *102*, 3202.
(54) Miller, W. H. *Annu. Rev. Phys. Chem.* **1990**, *41*, 245.
(55) Schatz, G. C. *J. Phys. Chem.* **1996**, *100*, 12839.
(56) Marcus, R. A.; Rice, O. K. *J. Phys. Colloid Chem.* **1951**, *55*, 894.
(57) Miller, W. H. *Proceedings of the Robert A. Welch Foundation 38th Conference on Chemical Research*; The Robert A. Welch Foundation, Austin, TX, 1994.
(58) Chatfield, D. C.; Friedman, R. S.; Truhlar, D. G.; Garrett, B. C.; Schwenke, D. W. *J. Am. Chem. Soc.* **1991**, *113*, 486.
(59) Seideman, T.; Miller, W. H. *J. Chem. Phys.* **1992**, *97*, 2499.
(60) Mielke, S. L.; Lynch, G. C.; Truhlar, D. G.; Schwenke, D. W. *J. Phys. Chem.* **1994**, *98*, 8000.
(61) Schinke, R. *Photodissociation Dynamics: Cambridge Monographs on Atomic, Molecular and Chemical Physics*; Cambridge University Press: New York, 1993; Vol. 1.
(62) Chen, I.-C.; Moore, C. B. *J. Phys. Chem.* **1990**, *94*, 269.
(63) Green, W. H.; Moore, C. B.; Polik, W. F. *Annu. Rev. Phys. Chem.* **1992**, *43*, 591.
(64) Katagiri, H.; Kato, S. *J. Chem. Phys.* **1993**, *99*, 8805.
(65) Pechukas, P.; Light, J. C. *J. Chem. Phys.* **1965**, *42*, 3281.
(66) Wardlaw, D. M.; Marcus, R. A. *Adv. Chem. Phys.* **1988**, *70*, 231.
(67) Truhlar, D. G.; Garrett, B. C. *Annu. Rev. Phys. Chem.* **1984**, *35*, 159.
(68) Quack, M.; Troe, J. *Int. Rev. Phys. Chem.* **1981**, *1*, 97.
(69) Green, W. H.; Mahoney, A. J.; Zheng, Q.-K.; Moore, C. B. *J. Chem. Phys.* **1991**, *94*, 1961.
(70) Klippenstein, S. J.; Marcus, R. A. *J. Chem. Phys.* **1989**, *91*, 2280.
(71) Allen, W. D.; Schaefer, H. F., III. *J. Chem. Phys.* **1986**, *84*, 2212.
(72) Allen, W. D.; Schaefer, H. F., III. *J. Chem. Phys.* **1988**, *89*, 329.
(73) Green, W. H.; Chen, I.-C.; Moore, C. B. *Ber. Bunsen-Ges. Phys. Chem.* **1988**, *92*, 389.
(74) Chen, I. C.; Green, W. H.; Moore, C. B. *J. Chem. Phys.* **1988**, *89*, 314.
(75) Garcia-Moreno, I.; Lovejoy, E. R.; Moore, C. B. *J. Chem. Phys.* **1994**, *100*, 8890, 8902.
(76) Polik, W. F.; Guyer, D. R.; Moore, C. B. *J. Chem. Phys.* **1990**, *92*, 3453.
(77) Abel, B.; Hamann, H. H.; Lange, N.; Troe, J. *J. Chem. Phys.*, in press.
(78) Choi, Y. S.; Moore, C. B. *J. Chem. Phys.* **1991**, *94*, 5414.
(79) Whitten, G. Z.; Rabinovitch, B. S. *J. Chem. Phys.* **1963**, *38*, 2466.
(80) Gezelter, D.; Miller, W. H. *J. Chem. Phys.* **1996**, *104*, 3546.
(81) Osborn, D. L.; Choi, H.; Neumark, D. M. *Adv. Chem. Phys.*, in press.
(82) Lovejoy, E. R.; Moore, C. B. *J. Chem. Phys.* **1993**, *98*, 7846.
(83) Russell, R. L.; Rowland, F. S. *J. Am. Chem. Soc.* **1970**, *92*, 7508.
(84) Scott, A. P.; Nobes, R. H.; Schaefer, H. F., III; Radom, L. *J. Am. Chem. Soc.* **1994**, *116*, 10159.
(85) Lovejoy, E. R.; Kim, S. K.; Alvarez, R. A.; Moore, C. B. *J. Chem. Phys.* **1991**, *95*, 4081.
(86) Gezelter, D.; Miller, W. H. *J. Chem. Phys.* **1995**, *103*, 7868.
(87) Kim, S. K.; Choi, Y. S.; Pibel, C. D.; Zheng, Q.-K.; Moore, C. B. *J. Chem. Phys.* **1991**, 1954.
(88) Potter, E. D.; Gruebele, M.; Khundkar, L. R.; Zewail, A. H. *Chem. Phys. Lett.* **1989**, *164*, 463.
(89) Yu, J.; Klippenstein, S. J. *J. Phys. Chem.* **1991**, *95*, 9882.
(90) Dashevskaya, E. I.; Nikitin, E. E.; Troe, J. *J. Chem. Phys.* **1992**, *97*, 3318.
(91) Maergoiz, A. I.; Nikitin, E. E.; Troe, J. *J. Chem. Phys.* **1991**, *95*, 5117.
(92) Klippenstein, S. J.; Khundkar, L. R.; Zewail, A. H.; Marcus, R. A. *J. Chem. Phys.* **1988**, *89*, 4761.
(93) Qian, C. X. W.; Ogai, A.; Reisler, H.; Wittig, C. *J. Chem. Phys.* **1989**, *90*, 209.
(94) Miyawaki, J.; Yamanouchi, K.; Tsuchiya, S. *J. Chem. Phys.* **1993**, *99*, 254.

(95) Ionov, S. I.; Davis, H. F.; Mikhaylichenko, K.; Valachovic, L.; Beaudet, R. A.; Wittig, C. *J. Chem. Phys.* **1994**, *101*, 4809.
(96) Brucker, G. A.; Ionov, S. I.; Chen, Y.; Wittig, C. *Chem. Phys. Lett.* **1992**, *194*, 301.
(97) Ionov, S. I.; Brucker, G. A.; Jaques, C.; Valachovic, L.; Wittig, C. *J. Chem. Phys.* **1993**, *99*, 6553.
(98) Reid, S. A.; Brandon, J. T.; Hunter, M.; Reisler, H. *J. Chem. Phys.* **1993**, *99*, 4860.
(99) Reid, S. A.; Robie, D. C.; Reisler, H. *J. Chem. Phys.* **1994**, *100*, 4256.
(100) Reid, S. A.; Reisler, H. *J. Chem. Phys.* **1994**, *101*, 5683.
(101) Abel, B.; Hamann, H. H.; Lange, N. *Faraday Discuss. Chem. Soc.*, in press.
(102) Troe, J. *Chem. Phys.* **1994**, *190*, 381.
(103) Polik, W. F.; Moore, C. B.; Miller, W. H. *J. Chem. Phys.* **1988**, *89*, 3584.
(104) Polik, W. F.; Guyer, D. R.; Moore, C. B.; Miller, W. H. *J. Chem. Phys.* **1990**, *92*, 3471.
(105) Hernandez, R.; Miller, W. H.; Moore, C. B.; Polik, W. F. *J. Chem. Phys.* **1993**, *99*, 950.
(106) Dertinger, S.; Geers, A.; Kappert, J.; Wiebrecht, J.; Temps, F. *Faraday Discuss. Chem. Soc.*, in press.
(107) Dobbyn, A. J.; Stumpf, M.; Keller, H.-M.; Hase, W. L.; Schinke, R. *J. Chem. Phys.* **1995**, *102*, 7070.
(108) Ambartzumian, R. V.; Gorokhov, Y. A.; Letokhov, V. S.; Makarov, G. N. *JETP Lett.* **1975**, *21*, 171.
(109) Lyman, J. L.; Jensen, R. J.; Rink, J.; Robinson, G. P.; Rockwood, D. S. *Appl. Phys. Lett.* **1975**, *27*, 87.
(110) Schulz, P. A.; Sudbo, A. S.; Krajnovich, D. J.; Kwok, H. S.; Shen, Y. R.; Lee, Y. T. *Annu. Rev. Phys. Chem.* **1979**, *30*, 379.
(111) He, Y.; Pochert, J.; Quack, M.; Ranz, R.; Seyfang, G. *Faraday Discuss. Chem. Soc.*, in press.
(112) Wyatt, R. E.; Iung, C.; Leforestier, C. *Acc. Chem. Res.* **1995**, *28*, 423.
(113) Field, R.; Nesbitt, D. J. *J. Phys. Chem.* **1996**, *100*, 12735.
(114) Neyer, D. W.; Houston, P. L. The HCO Potential Energy Surface; Probes using Molecular Scattering and Photodissociation. In *The Chemical Dynamics and Kinetics of Small Radicals*; Liu, K., Wagner, A., Eds.; World Scientific Publishers: Singapore, 1995.
(115) Werner, H. J.; Bauer, C.; Rosmus, P.; Keller, H.-M.; Stumpf, M.; Schinke, R. *J. Chem. Phys.* **1995**, *102*, 3593.
(116) Wang, D.; Bowman, J. M. *J. Chem. Phys.* **1994**, *100*, 1021.
(117) Choi, Y. S.; Moore, C. B. *J. Chem. Phys.* **1992**, *97*, 1010.
(118) Miller, W. H. *J. Am. Chem. Soc.* **1983**, *105*, 216.
(119) Graener, H.; Ye, T. Q.; Laubereau, A. *J. Chem. Phys.* **1989**, *91*, 1043.
(120) Graener, H.; Ye, T. Q.; Laubereau, A. *J. Chem. Phys.* **1989**, *90*, 3413.
(121) Smalley, R. E. *Annu. Rev. Phys. Chem.* **1983**, *34*, 129.
(122) Butenhoff, T. J.; Chuck, R. S.; Limbach, H.-H.; Moore, C. B. *J. Phys. Chem.* **1990**, *94*, 7847.
(123) Natzle, W. C.; Moore, C. B.; Goodall, D. M.; Frisch, W.; Holzwarth, J. F. *J. Phys. Chem.* **1981**, *85*, 2882.
(124) Parker, D. H.; Jalink, H.; Stolte, S. *J. Phys. Chem.* **1987**, *91*, 5427.
(125) Orr-Ewing, A. J.; Zare, R. N. *Annu. Rev. Phys. Chem.* **1994**, *45*, 15.
(126) Shin, S. K.; Chen, Y.; Nickolaisen, S.; Sharpe, S. W.; Beaudet, R. W.; Wittig, C. *Adv. Photochem.* **1991**, *16*, 249.
(127) Wittig, C.; Sharpe, S.; Beaudet, R. W. *Acc. Chem. Res.* **1988**, *88*, 341.
(128) Herschbach, D. R. *Faraday Discuss. Chem. Soc.* **1973**, *55*, 233.
(129) Carrington, T.; Polanyi, J. C. Chemical Kinetics. In *International Review of Science*.; Butterworths: London, 1972; Vol. 9.
(130) Schnieder, L.; Seekamp-Rahn, K.; Borkowski, J.; Wrede, E.; Welge, K. H.; Aoiz, F. J.; Bañares, L.; D'Mello, M. J.; Herrero, V. J.; Sáez Rábanos, V.; Wyatt, R. E. *Science (Washington, D.C.)* **1995**, *269*, 207.
(131) Xu, H.; Shafer-Ray, N. E.; Merkt, F.; Hughes, D. J.; Springer, M.; Tuckett, R. P.; Zare, R. N. *J. Chem. Phys.* **1995**, *103*, 5157.
(132) Liu, B. *J. Chem. Phys.* **1973**, *58*, 1925.
(133) Siegbahn, P.; Liu, B. *J. Chem. Phys.* **1978**, *68*, 2457.
(134) Blomberg, M. R. A.; Liu, B. *J. Chem. Phys.* **1985**, *82*, 1050.
(135) Truhlar, D. G.; Horowitz, C. J. *J. Chem. Phys.* **1978**, *68*, 2466.
(136) Truhlar, D. G.; Horowitz, C. J. *J. Chem. Phys.* **1979**, *71*, 1514.
(137) Geddes, J.; Krause, H. F.; Fite, W. L. *J. Chem. Phys.* **1970**, *52*, 3296.
(138) Perry, D. S.; Polanyi, J. C. *Chem. Phys.* **1976**, *12*, 419.
(139) Berry, M. J. *J. Chem. Phys.* **1973**, *59*, 6229.
(140) Schafer, T. P.; Siska, P. E.; Parson, J. M.; Tully, F. P.; Wong, Y. C.; Lee, Y. T. *J. Chem. Phys.* **1970**, *53*, 3385.
(141) Continetti, R. E.; Balko, B. A.; Lee, Y. T. *J. Chem. Phys.* **1990**, *93*, 5719.
(142) Zhang, J. Z. H.; Miller, W. H. *J. Chem. Phys.* **1989**, *91*, 1528.
(143) Zhao, M.; Truhlar, D. G.; Schwenke, D. W.; Kouri, D. J. *J. Phys.Chem.* **1990**, *94*, 7074.
(144) Kliner, D. A. V.; Rinnen, K.-D.; Zare, R. N. *Chem. Phys. Lett.* **1990**, *166*, 107.
(145) Adelman, D. E.; Shafer, N. E.; Kliner, D. A. V.; Zare, R. N. *J. Chem. Phys.* **1992**, *97*, 7323.
(146) Neuhauser, D.; Judson, R. S.; Kouri, D. J.; Adelman, D. E.; Shafer, N. E.; Kliner, D. A. V.; Zare, R. N. *Science (Washington, D.C.)* **1992**, *257*, 519.
(147) Adelman, D. E.; Xu, H.; Zare, R. N. *Chem. Phys. Lett.* **1993**, *203*, 573.
(148) Kitsopoulos, T. N.; Buntine, M. A.; Baldwin, D. P.; Zare, R. N.; Chandler, D. W. *Science (Washington, D.C.)* **1993**, *260*, 1605.
(149) Gerrity, G. P.; Valentini, J. J. *J. Chem. Phys.* **1984**, *81*, 1298.
(150) Phillips, D. C.; Levene, H. B.; Valentini, J. J. *J. Chem. Phys.* **1989**, *90*, 1600.
(151) Auerbach, S. M.; Miller, W. H. *J. Chem. Phys.* **1994**, *100*, 1103.
(152) Kneba, M.; Wellhausen, U.; Wolfrum, J. *Ber. Bunsen-Ges. Phys. Chem.* **1979**, *83*, 940.
(153) Dreier, T.; Wolfrum, J. *Int. J. Chem. Kinet.* **1986**, *18*, 919.
(154) Smith, I. W. M. *Acc. Chem. Res.* **1990**, *23*, 101.
(155) Garrett, B. C.; Truhlar, D. G. *J. Phys. Chem.* **1985**, *89*, 2204.
(156) Kuppermann, A.; Wu, Y.-S. M. *Chem. Phys. Lett.* **1993**, *205*, 577.
(157) Neumark, D. M.; Wodtke, A. M.; Robinson, G. N.; Hayden, C. C.; Lee, Y. T. *J. Chem. Phys.* **1985**, *87*, 3045.
(158) Neumark, D. M.; Wodtke, A. M.; Robinson, G. N.; Hayden, C. C.; Shobatake, K.; Sparks, R. K.; Schafer, T. P.; Lee, Y. T. *J. Chem. Phys.* **1985**, *82*, 3067.
(159) Bradforth, S. E.; Arnold, D. W.; Neumark, D. M.; Manolopoulos, D. E. *J. Chem. Phys.* **1993**, *99*, 6345.
(160) Manolopoulos, D. E.; Stark, K.; Werner, H.-J.; Arnold, D. W.; Bradforth, S. E.; Neumark, D. M. *Science (Washington, D.C.)* **1993**, *262*, 1852.
(161) Knowles, P. J.; Stark, K.; Werner, H.-J. *Chem. Phys. Lett.* **1991**, *185*, 555.
(162) Castillo, J. F.; Manolopoulos, D. E.; Stark, K.; Werner, H.-J. Submitted to *J. Chem. Phys*.
(163) Germann, G. J.; Huh, Y.-D.; Valentini, J. J. *J. Chem. Phys.* **1991**, *95*, 1957.
(164) Aker, P. M.; Germann, G. J.; Valentini, J. J. *J. Chem. Phys.* **1992**, *96*, 2756.
(165) Germann, G. J.; Huh, Y.-D.; Valentini, J. J. *J. Chem. Phys.* **1992**, *96*, 5746.
(166) Lanzisera, D. V.; Valentini, J. J. *Chem. Phys. Lett.* **1993**, *216*, 122.
(167) Aker, P. M.; Valentini, J. J. *J. Chem. Phys.* **1993**, *97*, 2078.
(168) Crim, F. F. *J. Phys. Chem.* **1996**, *100*, 12725.
(169) Varley, D. F.; Dagdigian, P. J. *J. Phys. Chem.* **1995**, *99*, 9843.
(170) Simpson, W. R.; Orr-Ewing, A. J.; Zare, R. N. *Chem. Phys. Lett.* **1993**, *212*, 163.
(171) Andresen, P.; Luntz, A. C. *J. Chem. Phys.* **1980**, *72*, 5842.
(172) Clary, D. C. *J. Phys. Chem.* **1994**, *98*, 10678.
(173) Schatz, G. C. *J. Phys. Chem.* **1995**, *99*, 516.
(174) Zhang, D. H.; Zhang, J. Z. H.; Zhang, Y.; Wang, D.; Zhang, Q. *J. Chem. Phys.* **1995**, *102*, 7400.
(175) Thompson, W. H.; Miller, W. H. *J. Chem. Phys.* **1994**, *101*, 8620.
(176) Schatz, G. C.; Elgersma, H. *Chem. Phys. Lett.* **1980**, *73*, 21.
(177) Light, G. C.; Matsumoto, J. H. *Chem. Phys. Lett.* **1978**, *58*, 578.
(178) Zellner, R.; Steinert, W. *Chem. Phys. Lett.* **1981**, *81*, 568.
(179) Glass, G. P.; Chaturvedi, B. K. *J. Chem. Phys.* **1981**, *75*, 2749.
(180) Cannon, B. D.; et al. *Chem. Phys. Lett.* **1984**, *105*, 380.
(181) Sims, I. R.; et al. *Chem. Phys. Lett.* **1988**, *149*, 565.
(182) Sims, I. R.; et al. *J. Chem. Soc., Faraday Trans.* **1989**, *85*, 915.
(183) Frost, M. J.; Smith, I. W. M.; Spencer-Smith, R. D. *Faraday Discuss. Chem. Soc.* **1993**, *89*, 2355.
(184) Alagia, M.; Balucani, N.; Casavecchia, P.; Stranges, D.; Volpi, G. G. *J. Chem. Phys.* **1993**, *98*, 2459.
(185) Butkovskaya, N. I.; Sester, D. W. *J. Phys. Chem.* **1996**, *100*, 4853.
(186) Bethardy, G. A.; Northrop, F. J.; Macdonald, R. G. *J. Chem. Phys.* **1995**, *103*, 2863.
(187) Smith, I. W. M. *Int. J. Mass. Spectrom. Ion Processes* **1995**, *149/150*, 231.
(188) Clary, D. C. *Annu. Rev. Phys. Chem.* **1990**, *41*, 61.
(189) Kleinermanns, K.; Schinke, R. *J. Chem. Phys.* **1984**, *80*, 1440.
(190) Kleinermanns, K.; Wolfrum, J. *J. Chem. Phys.* **1984**, *80*, 1446.
(191) Kleinermanns, K.; Linnebach, E. *Appl. Phys. B* **1985**, *36*, 203.
(192) Smith, I. W. M.; Tuckett, R. P.; Whitham, C. J. *J. Chem. Phys.* **1993**, *98*, 6267.
(193) Guadagnini, R.; Schatz, G. C.; Walch, S. P. *J. Chem. Phys.* **1995**, *102*, 774.
(194) Irvine, A. M. L.; Smith, I. W. M.; Tuckett, R. P.; Yang, X.-F. *J. Chem. Phys.* **1990**, *93*, 3177.
(195) Irvine, A. M. L.; Smith, I. W. M.; Tuckett, R. P. *J. Chem. Phys.* **1990**, *93*, 3187.
(196) Phillips, L. F.; Smith, I. W. M.; Tuckett, R. P.; Whitham, C. J. *Chem. Phys. Lett.* **1991**, *183*, 254.
(197) Sauder, D. G.; Dagdigian, P. J. *J. Chem. Phys.* **1991**, *95*, 1696.

(198) Sonnenfroh, D. M.; Macdonald, R. G.; Liu, K. *J. Chem. Phys.* **1990**, *93*, 1478.
(199) Smith, I. W. M. In *The Chemical Kinetics and Dynamics of Small Radicals*; Liu, K., Wagner, A. F., Eds.; World Scientific: Singapore, 1995.
(200) Clough, P. N.; Polanyi, J. C.; Taguchi, R. T. *Can. J. Chem.* **1970**, *48*, 2919.
(201) Brunning, J.; Derbyshire, D. W.; Smith, I. W. M.; Williams, M. D. *J. Chem. Soc., Faraday Trans. 2* **1988**, *84*, 105.
(202) Fulle, D.; Hamann, H. F.; Hippler, H.; Troe, J. *J. Chem. Phys.*, in press.
(203) Schatz, G. C.; Fitzcharles, M. S.; Harding, L. B. *Faraday Discuss. Chem. Soc.* **1987**, *84*, 359.
(204) Frost, M. J.; Salh, J. S.; Smith, I. W. M. *Faraday Discuss. Chem. Soc.* **1991**, *87*, 1037.
(205) Frost, M. J.; Sharkey, P.; Smith, I. W. M. *Faraday Discuss. Chem. Soc.* **1991**, *91*, 305.
(206) Jacobs, A.; Wahl, M.; Weller, R.; Wolfrum, J. *Chem. Phys. Lett.* **1989**, *158*, 161.
(207) Jacobs, A.; Volpp, H.-R.; Wolfrum, J. *Chem. Phys. Lett.* **1994**, *218*, 51.
(208) Radhakrishan, G.; Beulow, S.; Wittig, C. *J. Chem. Phys.* **1986**, *84*, 727.
(209) Nickolaisen, S. L.; Cartland, H. E.; Wittig, C. *J. Chem. Phys.* **1992**, *96*, 4378.
(210) Scherer, N. F.; Khundkar, L. R.; Bernstein, R. B.; Zewail, A. H. *J. Chem. Phys.* **1987**, *87*, 1451.
(211) Scherer, N. F.; Sipes, C.; Bernstein, R. B.; Zewail, A. H. *J. Chem. Phys.* **1990**, *92*, 1990.
(212) Brucker, G. A.; Jaques, C.; Valachovic, L.; Wittig, C. *J. Chem. Phys.* **1992**, *97*, 9486.
(213) Jaques, C.; Valachovic, L.; Ionov, S. I.; Bohmer, E.; Wen, Y.; Segall, J.; Wittig, C. *Faraday Discuss. Chem. Soc.* **1993**, *89*, 1419.
(214) Frost, M. J.; Sharkey, P.; Smith, I. W. M. *J. Phys. Chem.* **1993**, *97*, 12254.
(215) Bohmer, E.; Shin, S. K.; Chen, Y.; Wittig, C. *J. Chem. Phys.* **1992**, *97*, 2536.
(216) Ionov, S. I.; Ionov, P. I.; Wittig, C. *Faraday Discuss. Chem. Soc.* **1994**, *97*, 391.
(217) Costen, M. L.; Hancock, G.; Orr-Ewing, A. J.; Summerfield, D. *J. Chem. Phys.* **1994**, *100*, 2754.
(218) Brouard, M.; Duxon, S. P.; Enriquez, P. A.; Simons, J. P. *J. Chem. Phys.* **1992**, *97*, 7414.
(219) Brouard, M.; Lambert, H. M.; Short, J.; Simons, J. P. *J. Phys. Chem.* **1995**, *99*, 13571.
(220) Brouard, M.; Lambert, H. M.; Russell, C. L.; Short, J.; Simons, J. P. *Faraday Discuss. Chem. Soc.*, in press.
(221) Sathyamurthy, N. *Chem. Rev.* **1983**, *83*, 601.
(222) Altkorn, R.; Bartoszek, F. E.; Dehaven, J.; Hancock, G.; Perry, D. S.; Zare, R. N. *Chem. Phys. Lett.* **1983**, *98*, 212.
(223) Zhang, R.; Rakestraw, D. J.; McKendrick, K. G.; Zare, R. N. *J. Chem. Phys.* **1988**, *89*, 6283.
(224) Rettner, C. T.; Auerbach, D.; Tully, J.; Kleyn, A. *J. Phys. Chem.* **1996**, *100*, 13021.

JP953664H